HZB Helmholtz Zentrum Berlin

SoNS 2014

Neutron imaging – Data and image analysis

Nikolay Kardjilov

Principle of the conventional tomography

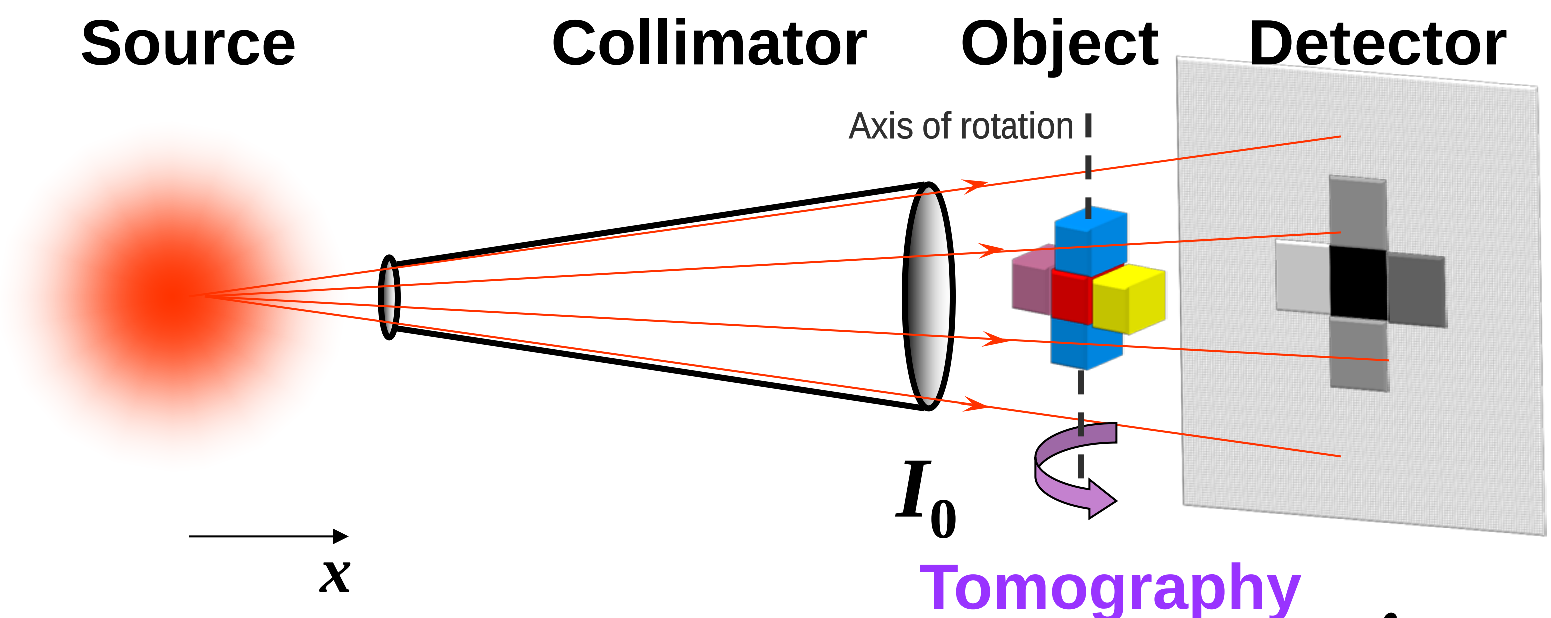

$$\sim I_0 e^{-\int \Sigma(x)dx}$$

x – propagation direction

I_0 – primary beam

$\Sigma(x)$ – attenuation coefficient

Absorption tomography

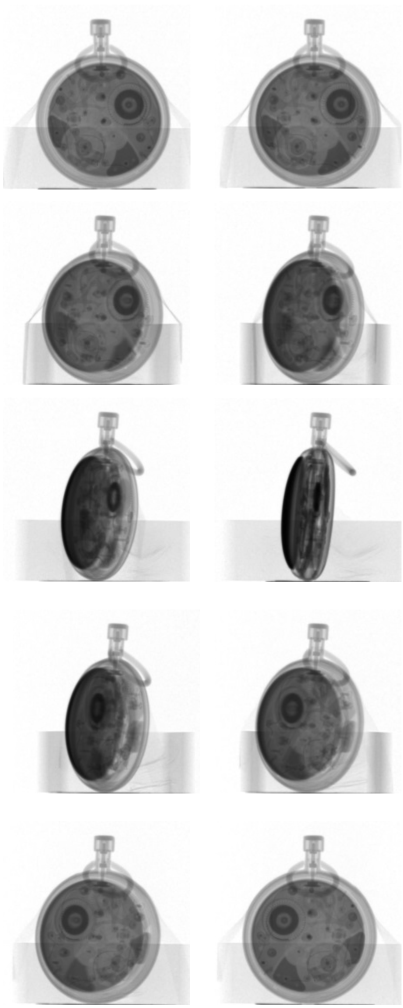

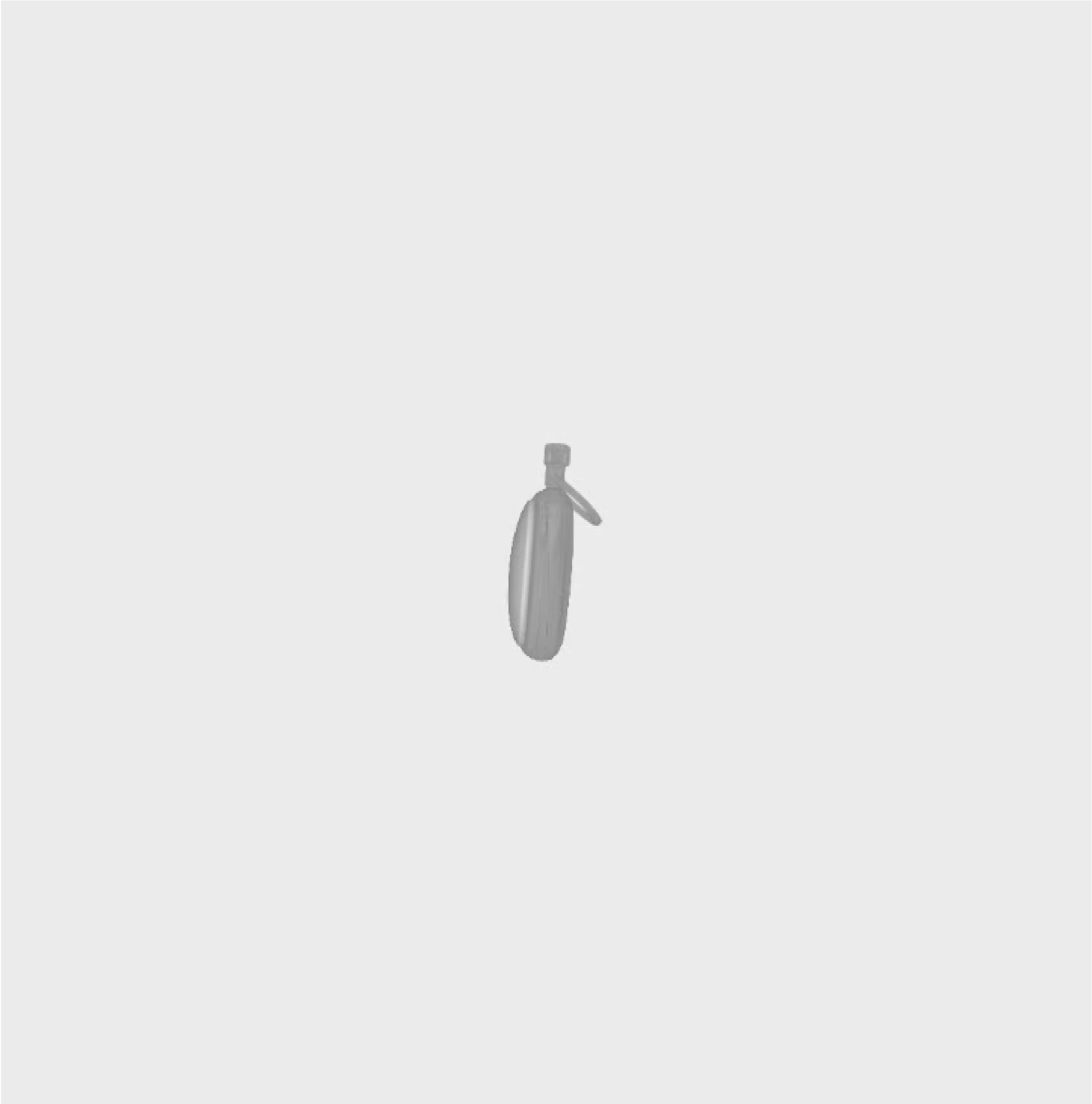

Measurement

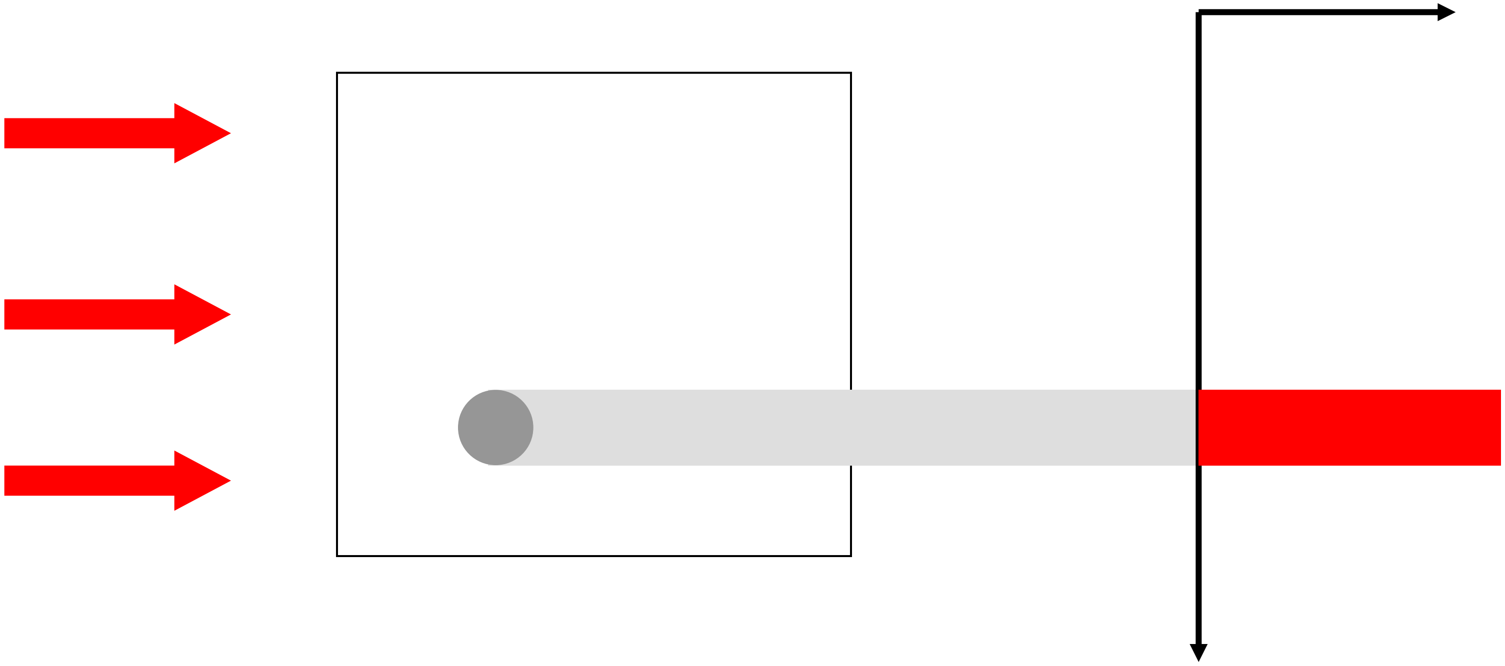

Measurement

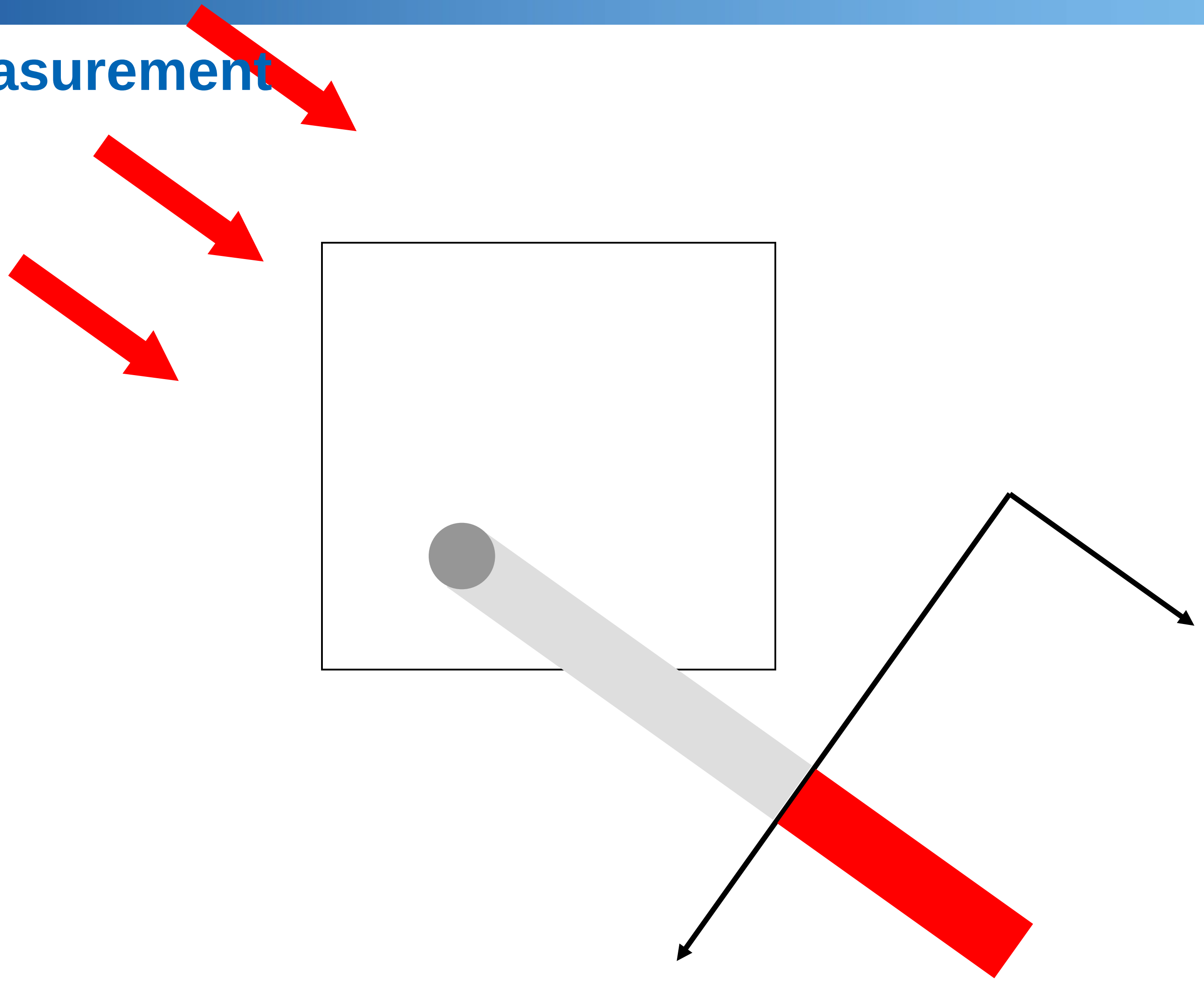

Measurement

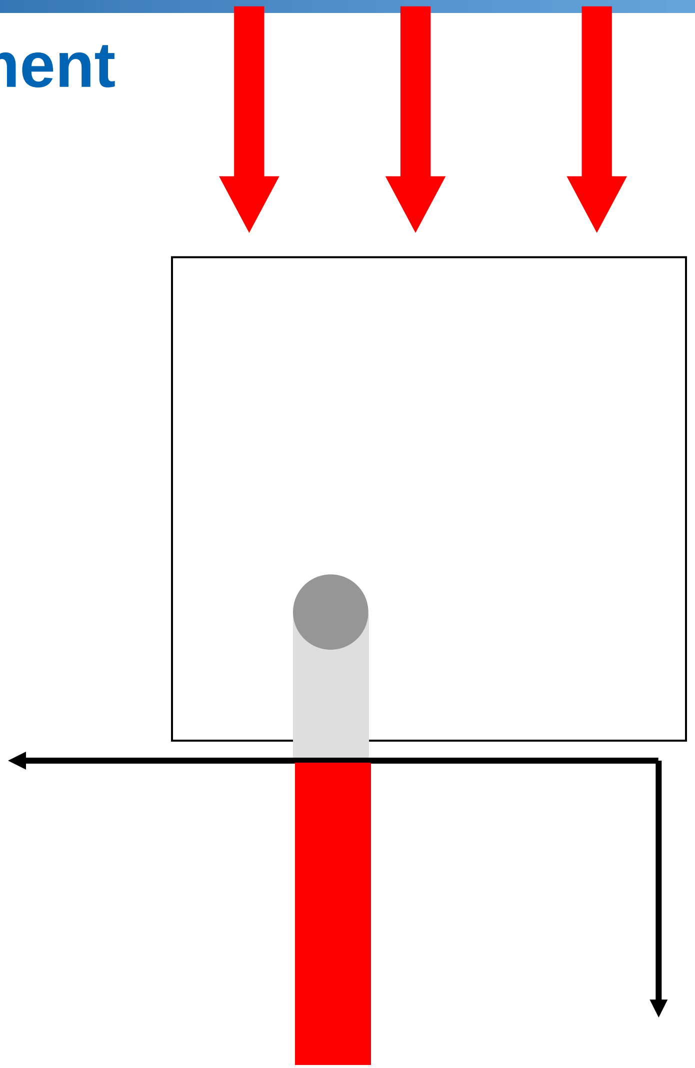

Back projection

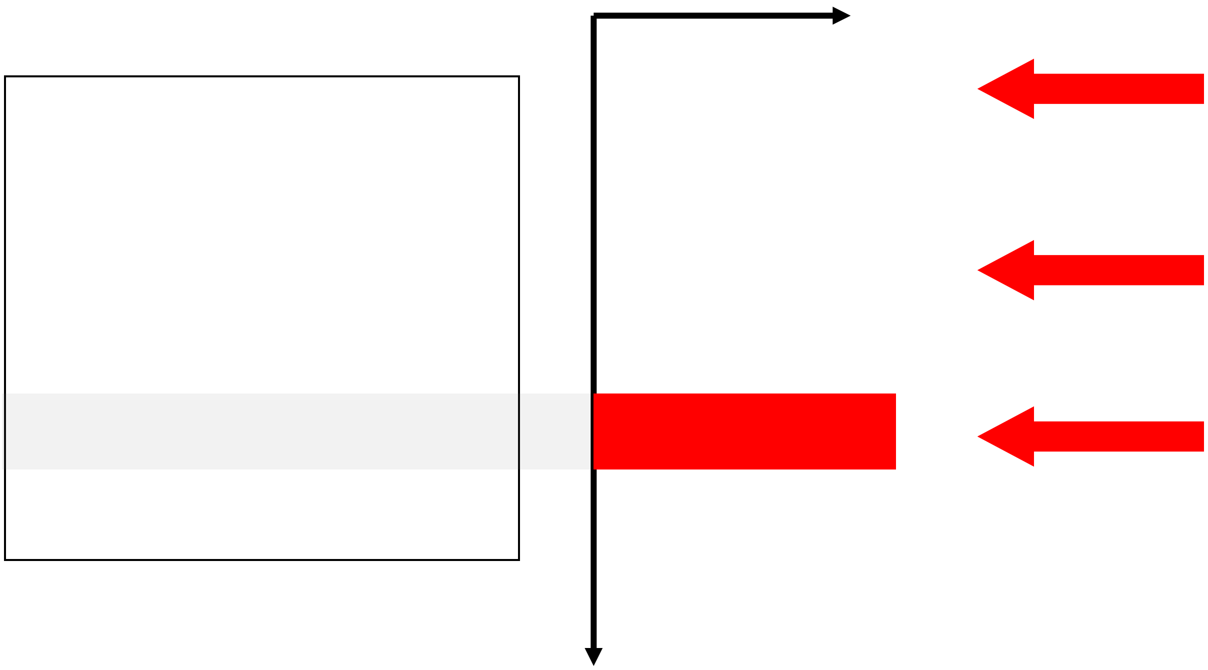

Back projection

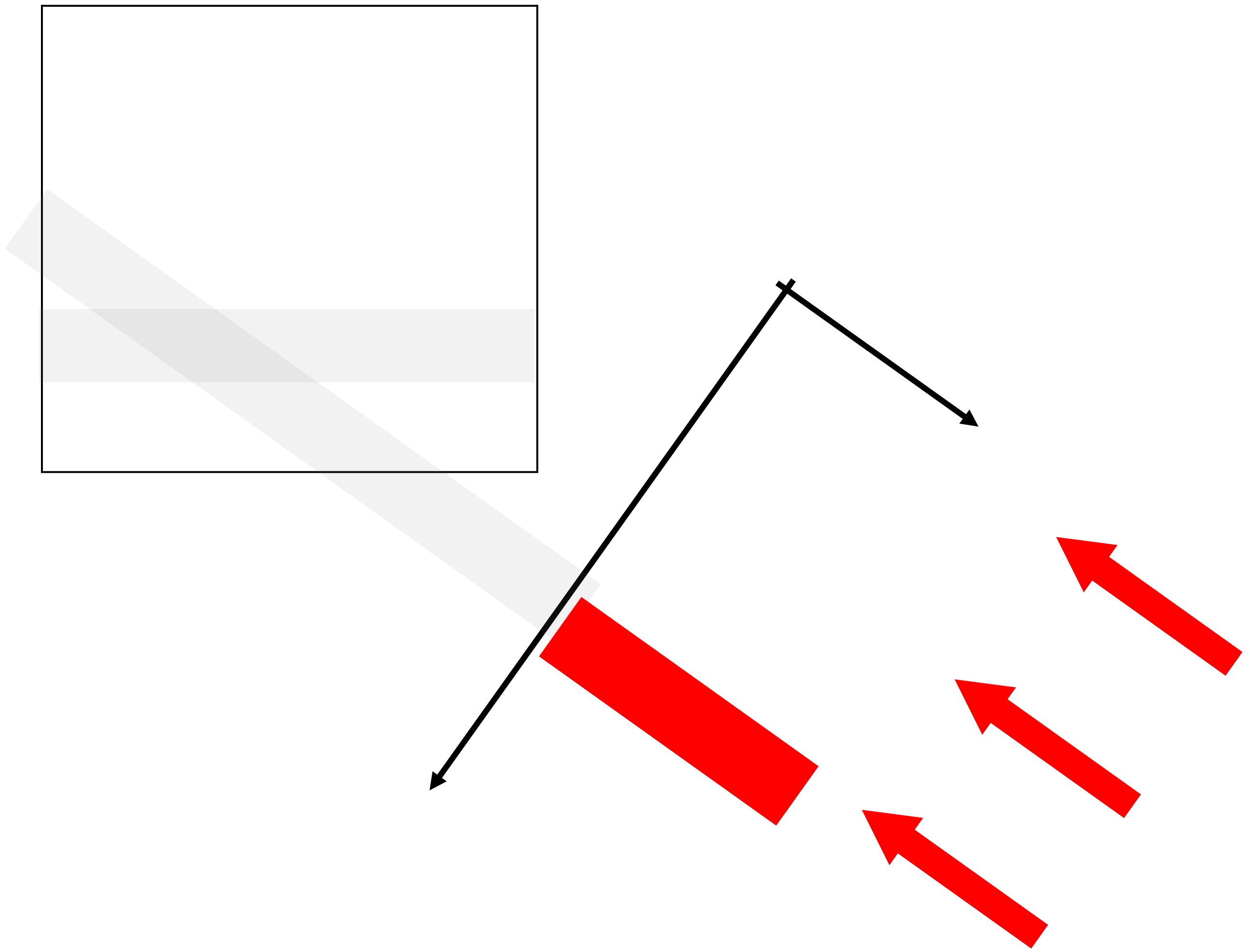

Back projection

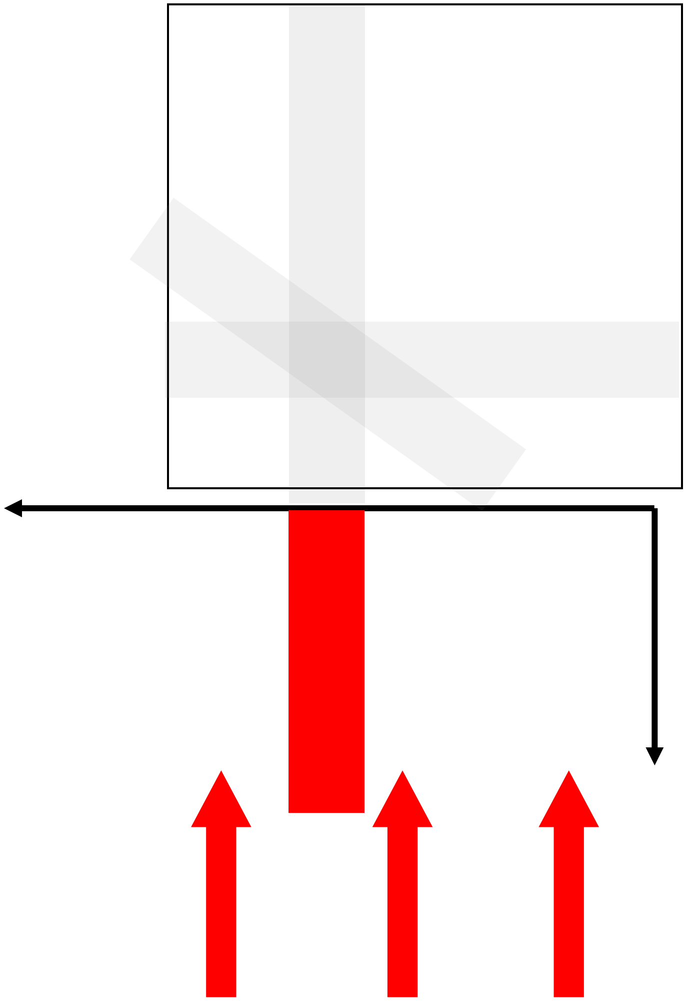

Back projection

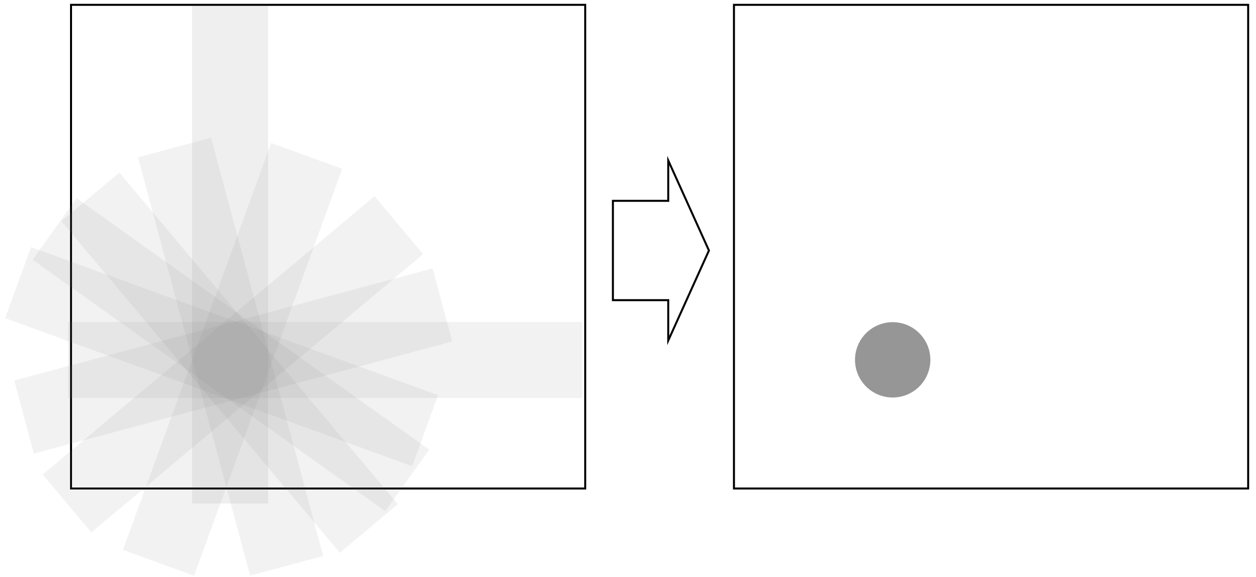

Neutron tomography - principle

Definition:

Tomography is the process of reconstructing a three dimensional distribution of the attenuation coefficients in the volume from many two dimensional projections of the sample, taken at different angles.

Assumptions:

1. 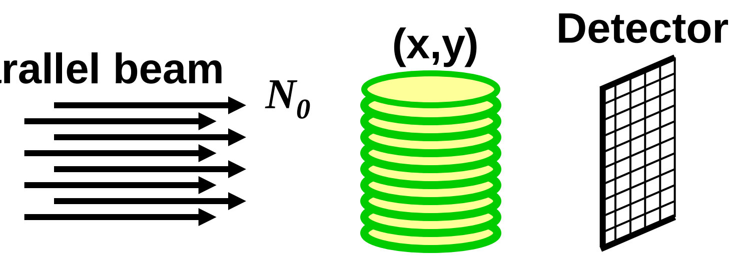

SAMPLE = SLICES

2. 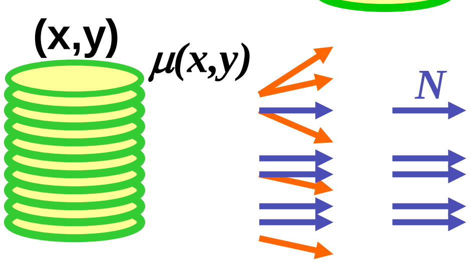

SCATTERING = ABSORPTION

$$N = N_0 \exp\left\{ - \int_{\text{beam path}} \mu(x,y)\,ds \right\}$$

3. 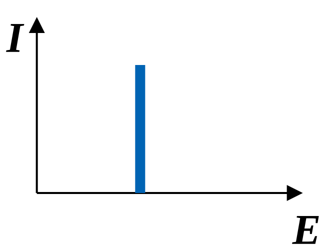

MONOENERGETIC BEAM

$$N = N_0 \exp\left\{ - \int_{\substack{beam\\path}} \mu(x,y)\,ds \right\}$$

$$p_\theta(t) = -\ln \frac{N_\theta(t)}{N_0(t)} = \int_{ray(\theta,t)} \mu(x,y)\,ds =$$

$$= \int_{-\infty}^{+\infty}\int_{-\infty}^{+\infty} \delta(x\cos\theta + y\sin\theta - t)\,\mu(x,y)\,dx\,dy$$

, where $t = x\cos\theta + y\sin\theta$

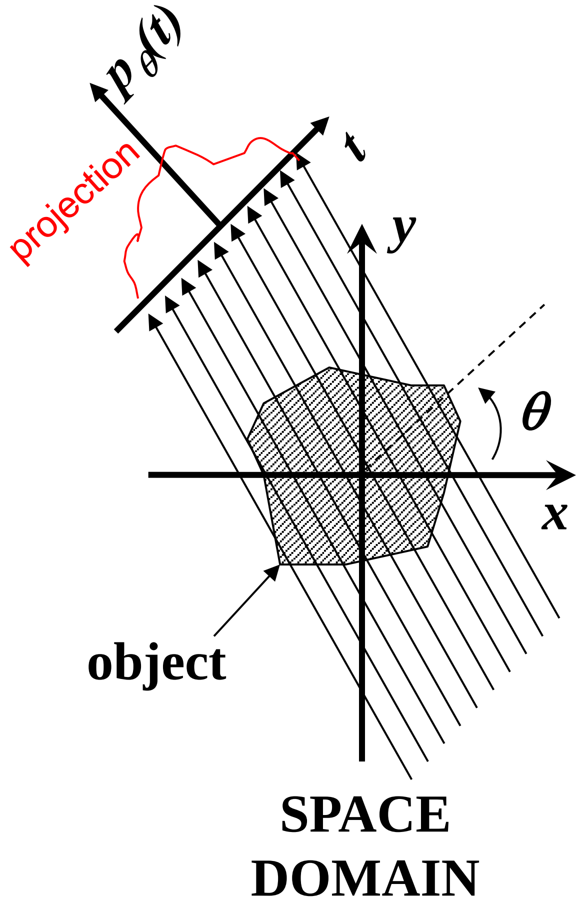

$$N = N_0 \exp\left\{-\int_{\substack{beam\\path}} \mu(x,y)ds\right\}$$

$$p_\theta(t) = -\ln\frac{N_\theta(t)}{N_0(t)} = \int_{ray(\theta,t)} \mu(x,y)ds =$$

$$= \int_{-\infty}^{+\infty}\int_{-\infty}^{+\infty} \delta(x\cos\theta + y\sin\theta - t)\mu(x,y)dxdy$$

, where $t = x\cos\theta + y\sin\theta$

$$P_\theta(\omega) = \int_{-\infty}^{+\infty} p_\theta(t)e^{-2\pi i\omega t}dt$$

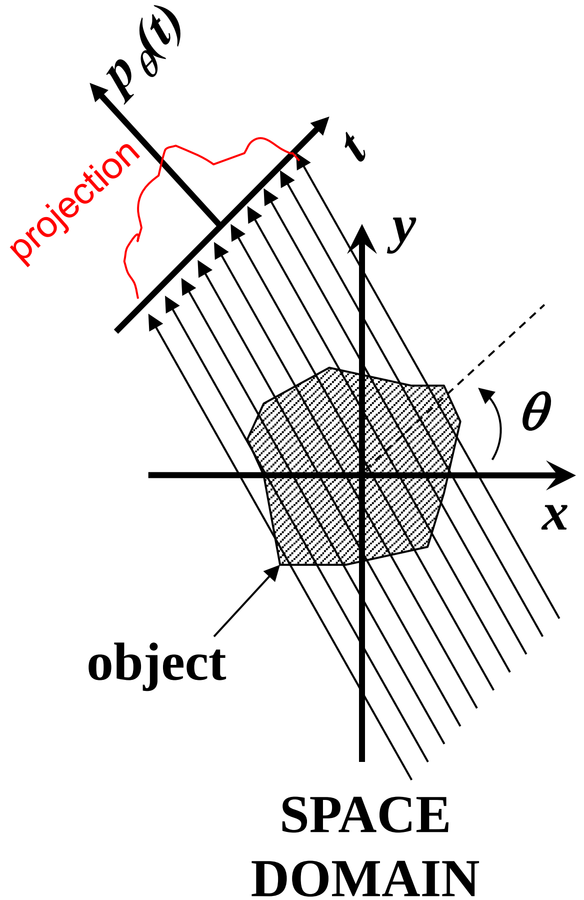

$$P_\theta(\omega) = \int_{-\infty}^{+\infty} p_\theta(t) e^{-2\pi i\omega t} dt$$

$$S(u,v) = \int_{-\infty}^{+\infty}\int_{-\infty}^{+\infty} \mu(x,y) e^{-2\pi i(ux+vy)} dxdy$$

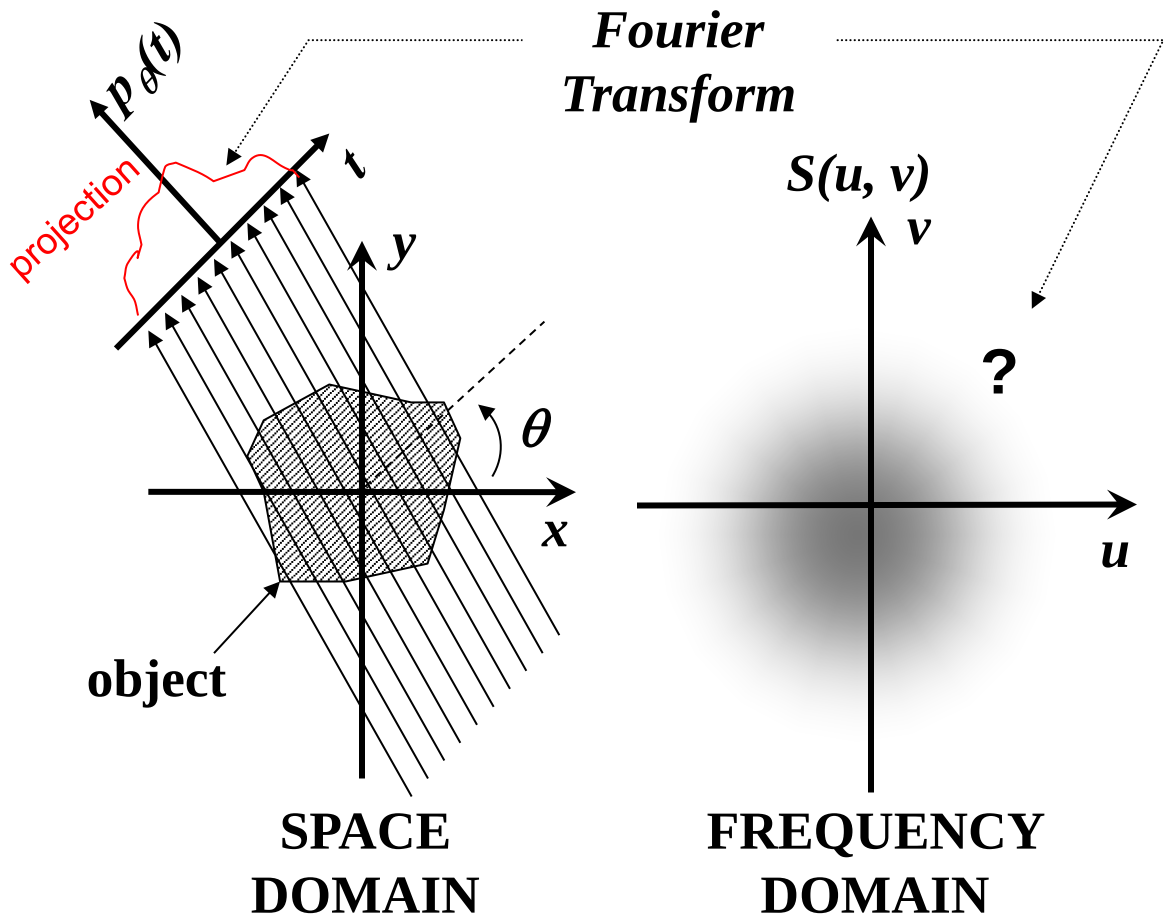

$$P_\theta(\omega) = \int_{-\infty}^{+\infty} p_\theta(t) e^{-2\pi i\omega t} dt$$

Fourier Slice Theorem $P_\theta(\omega) = S(\omega\cos\theta, \omega\sin\theta) \equiv S(\omega,\theta)$

$$S(u,v) = \int_{-\infty}^{+\infty}\int_{-\infty}^{+\infty} \mu(x,y) e^{-2\pi i(ux+vy)} dxdy$$

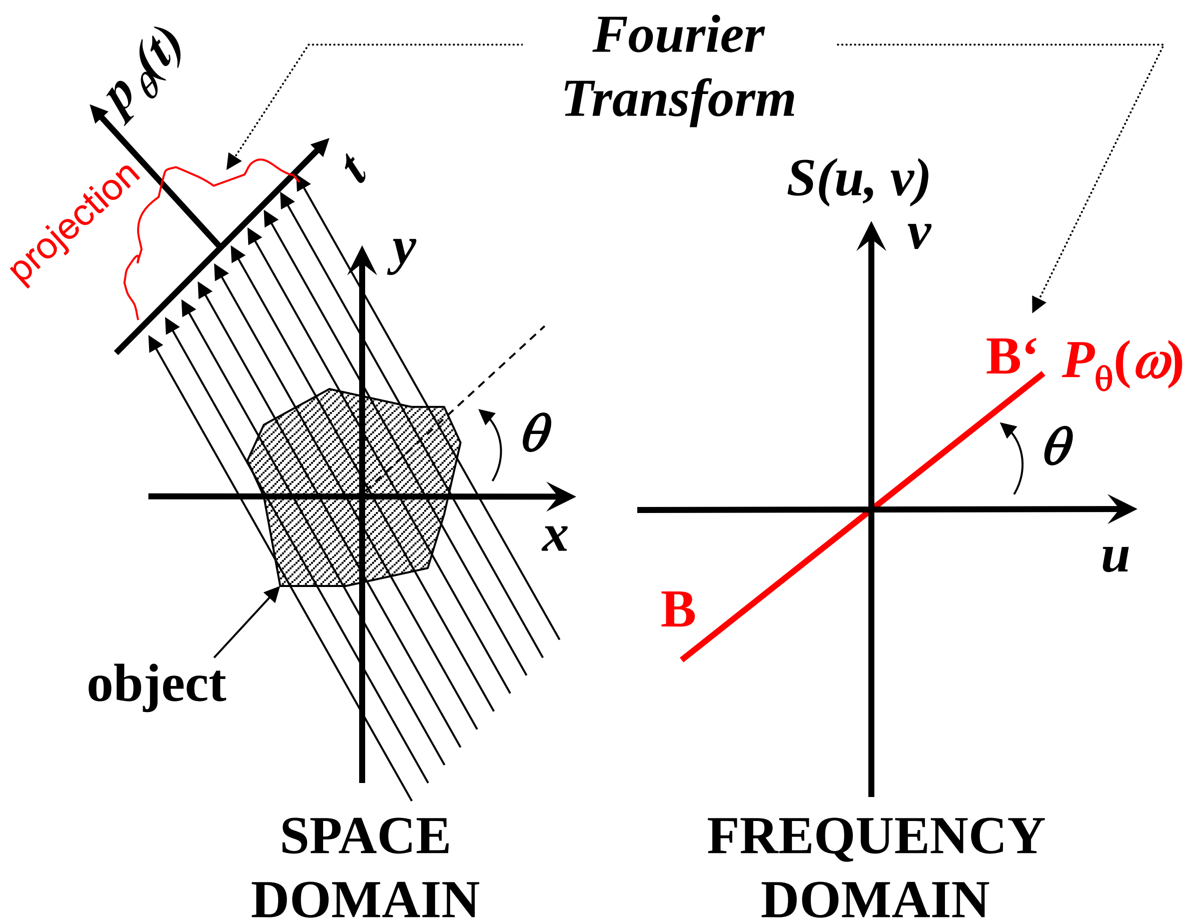

$$\mu(x,y) = \int_{-\infty}^{+\infty}\int_{-\infty}^{+\infty} S(u,v)e^{-2\pi i(ux+vy)}dudv$$

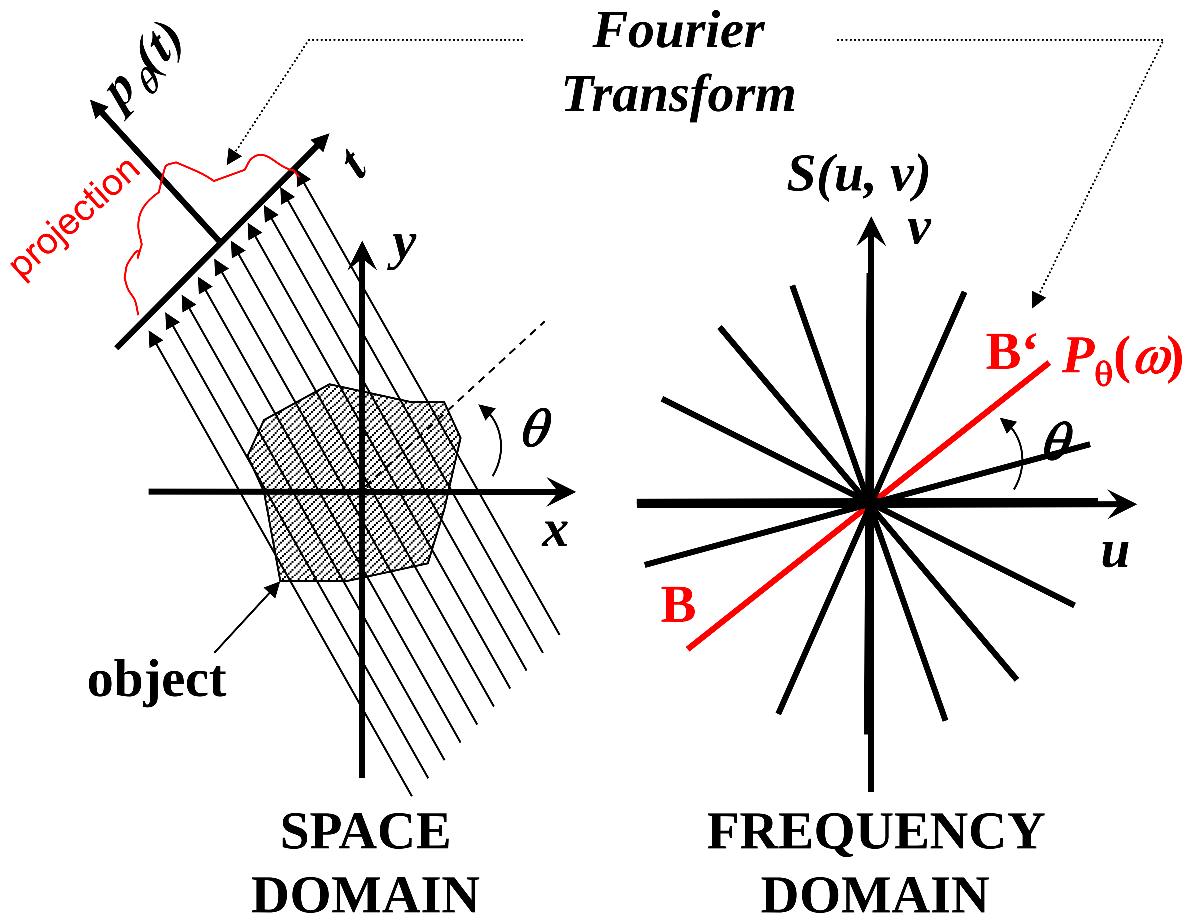

2.3 *Filtered Back-projection*

In reality, the number of rays and the number of projections is limited. The function S(u,v) is known only at a few points on radial lines.

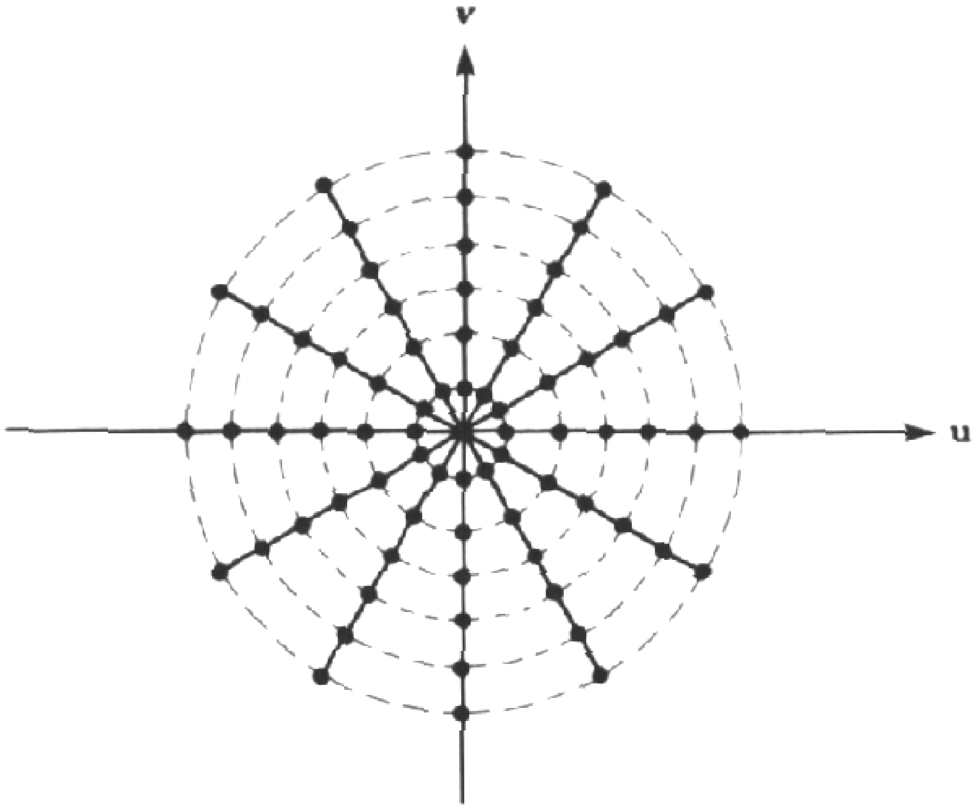

Measured values in frequency domain

- These points must be interpolated to a quadratic mesh.

- With increasing radial distance, the density of measured values decreases, and interpolation incertainty increases.

- A simple reconstruction can be performed by simply summing up the two-dimensional Fourier Transforms of the single lines.

- Because of the linearity of the Fourier Transform, this can be done either in spatial or in frequency domain.

- But as the density of measured values decreases towards high frequencies, the high frequencies do not get enough weight, and the reconstructed image appears smoothed or smeared.

Each of k projections over 180° must deliver the information for a "cake slice" of width $2\pi|\omega|/k$.

But as it delivers only a single line, it is weighted with a ramp filter of height $2\pi|\omega|/k$, so that the new wedge has the same "mass" as the cake slice.

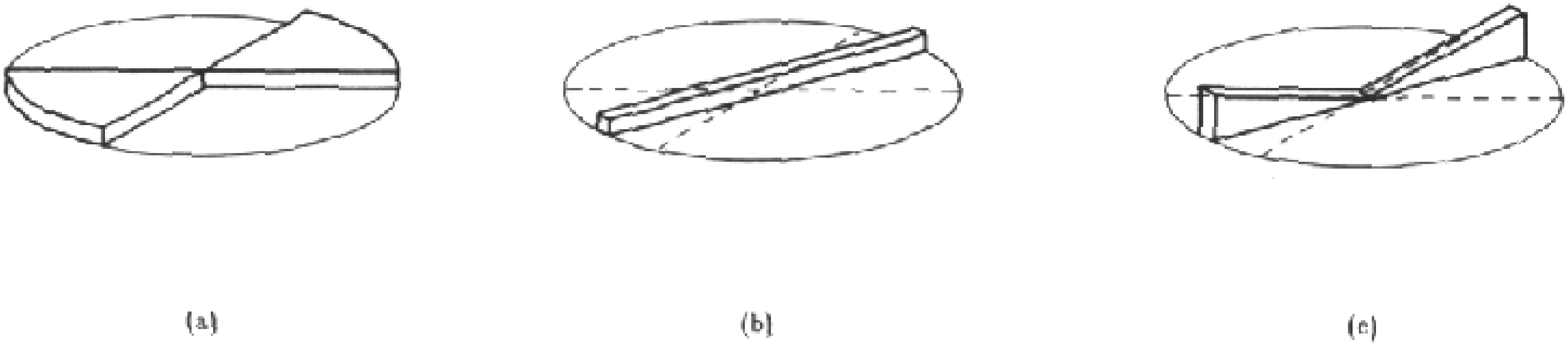

required, real and filtered representation
of the data in frequency domain

The filter |ω| can be obtained mathematically exact by transformation to polar coordinates in frequency space. Then we obtain

$$\Sigma(x,y) = \int_0^{\pi} \int_0^{+\infty} S(\omega,\theta) e^{2\pi i \omega (x\cos\theta + y\sin\theta)} |\omega| \, d\omega \, d\theta$$

$$= \int_0^{\pi} \int_0^{+\infty} S(\omega,\theta) e^{2\pi i \omega t} |\omega| \, d\omega \, d\theta \qquad \textit{with} \quad t = x\cos\theta + y\sin\theta$$

If we now substitute the one-dimensional Fourier Transform $P_\theta(\omega)$ of the projection at angle θ for the two-dimensional Fourier Transform S(ω,θ), we obtain

$$\Sigma(x,y) = \int_0^{\pi} \left[\int_0^{+\infty} P_\theta(\omega) e^{2\pi i \omega t} |\omega| \, d\omega \right] d\theta \qquad \textit{with} \quad t = x\cos\theta + y\sin\theta$$

$$= \int_0^{\pi} Q_\theta(x\cos\theta + y\sin\theta) \, d\theta \qquad \textit{with} \quad Q_\theta(t) = \int_0^{+\infty} P_\theta(\omega) e^{2\pi i \omega t} |\omega| \, d\omega$$

This Equation describes a filter operation with the filter |ω|.

The simple multiplication of $P_\theta(\omega)$ by ω in the frequency domain can be replaced by a convolution of $p_\theta(t)$ with the Fourier Transform of $|\omega|$ in the spatial domain:

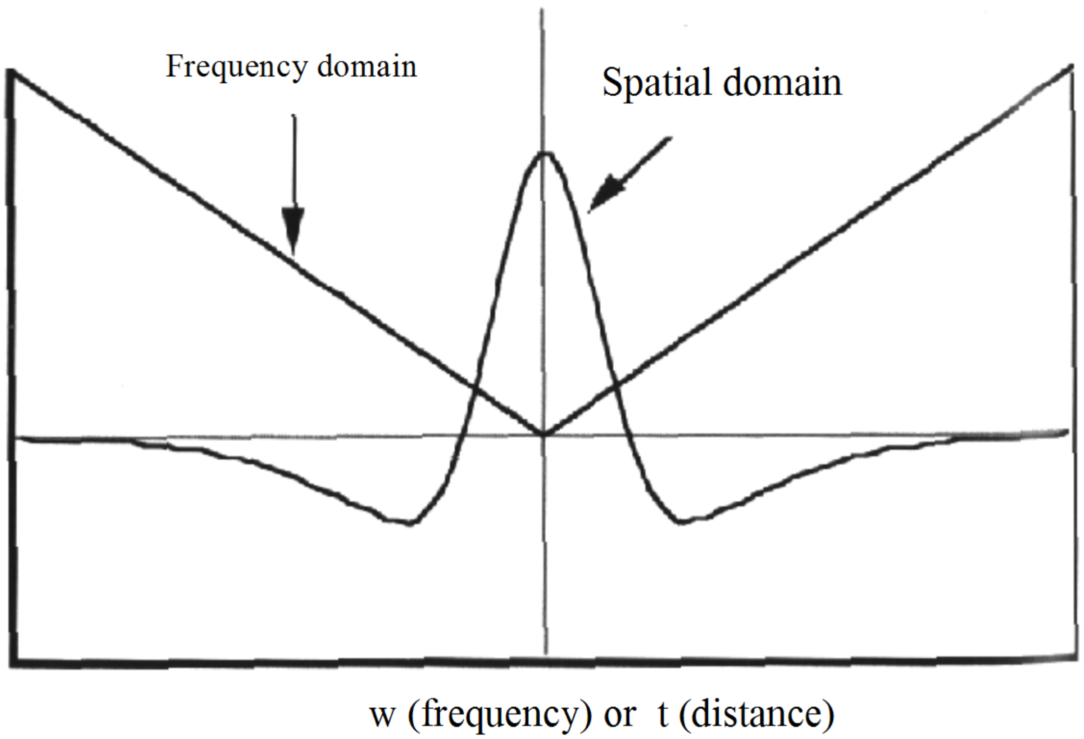

The ideal filter $|\omega|$ in spatial and frequency domain

- The value of each raysum is shared out equally among all the voxels through which the ray passed. This is called backprojection.

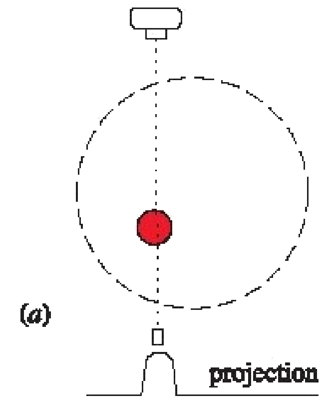

- As such an image is formed, albeit a poor one. An unwanted star-burst pattern is obtained.

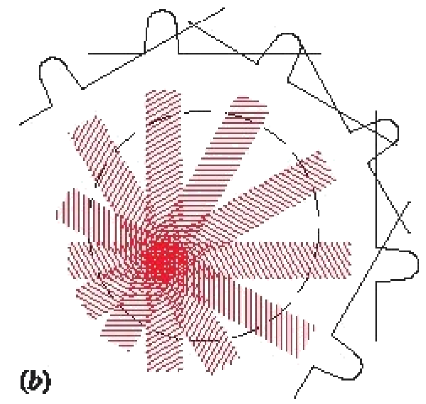

- The attenuation profile is convolved with a filter function prior to back-projection.

- The action of the filter is such that the starburst pattern disappears and an accurate representation of the original object is obtained.

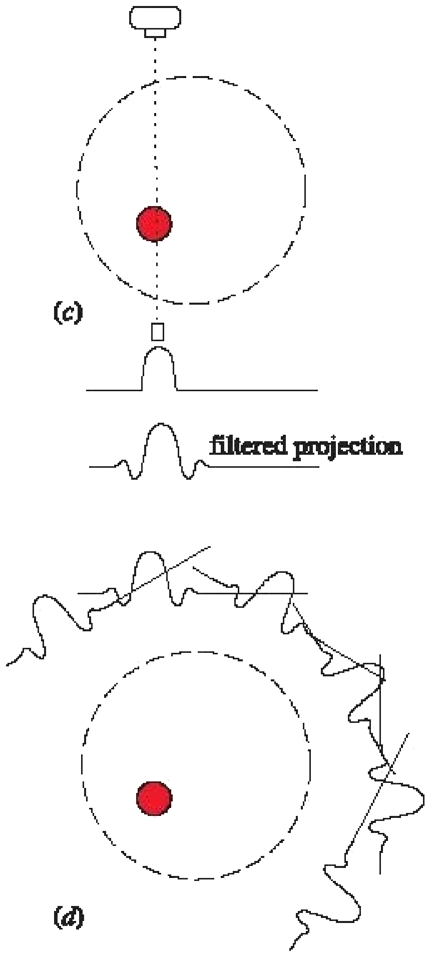

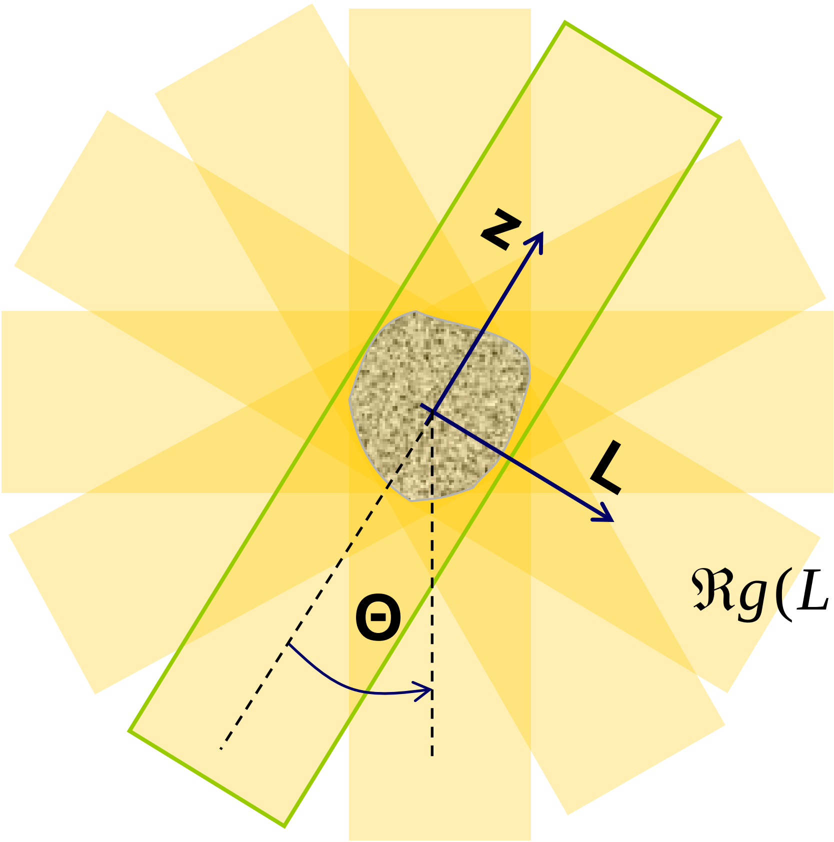

Object in polar coordinates:

$$g(r,\varphi) = g\left(\sqrt{L^2+z^2}, \tan^{-1}(z/L)\right)$$

Radon Transform of object:

$$\Re g(L,\Theta) = \int_{-\infty}^{+\infty} g\left(\sqrt{L^2+z^2}, \Theta + \tan^{-1}(z/L)\right) dz$$

Filtered Back Projection:

$$\mathrm{B}[\Re g](r,\varphi) = \int_0^{\pi} \left(\Re g(L,\Theta) * k(L)\right)_L d\theta$$

Back Projection **Filter**

… then we have to take into account the discrete pixels!

The filtered back-projection is being "smeared" along the original ray path across the reconstruction field.

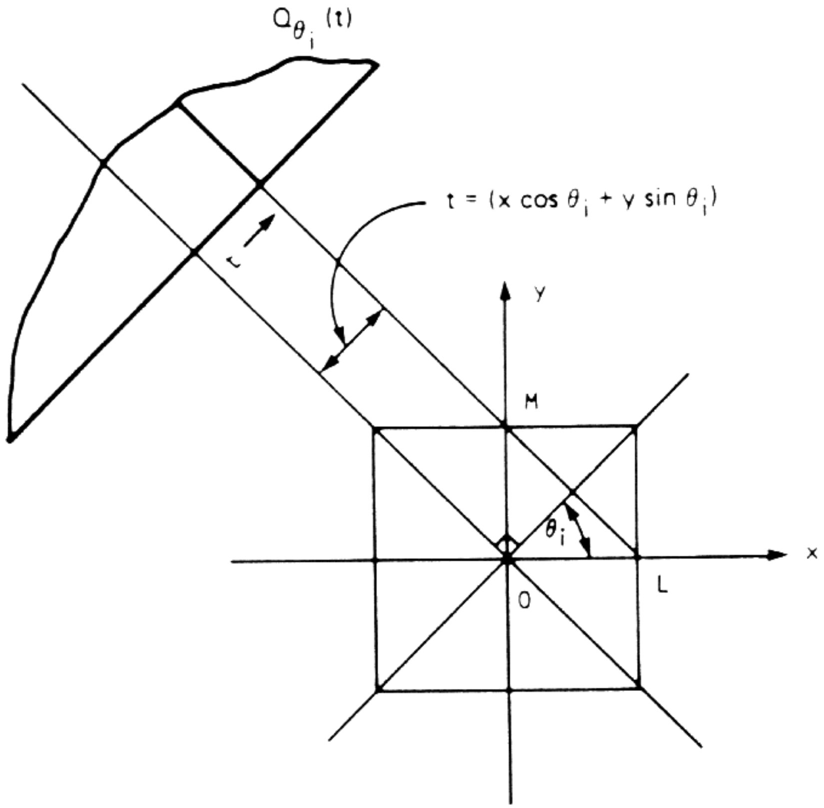

Back-projection of filtered data

•Difficulties with the ideal filter |ω| occur with noisy data, as noise consists mainly of high frequencies, which are much enhanced by this filter.
•The ideal filter is therefore often replaced by special filter functions that decrease again towards high frequencies.
•For neutrons, the inherent beam unsharpness (see below) often attenuates most high frequencies towards the Nyquist limit.

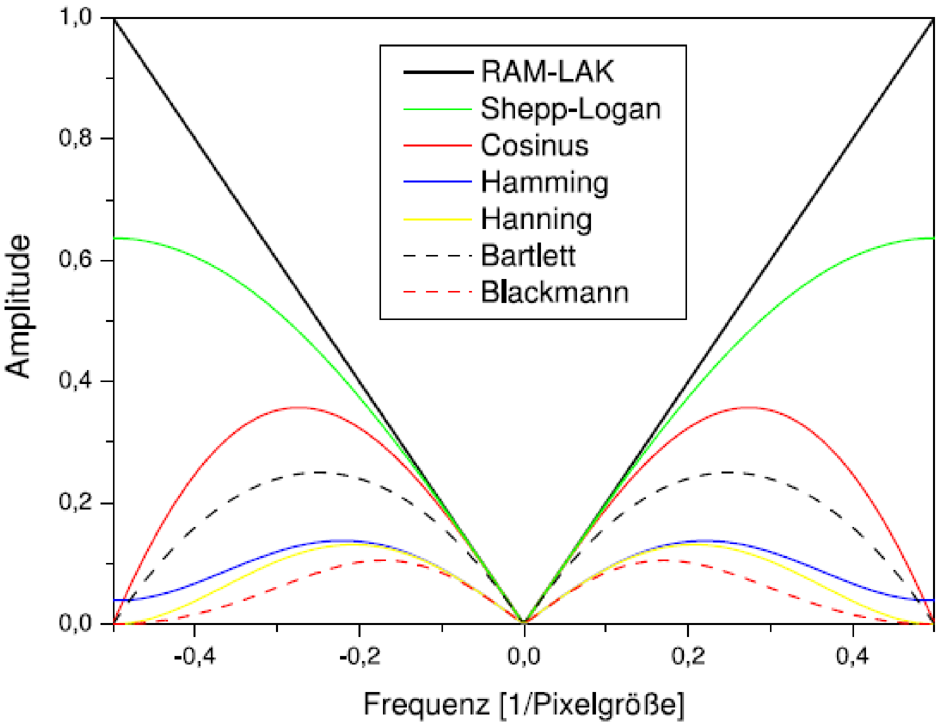

The ideal filter |ω| and some alternative functions

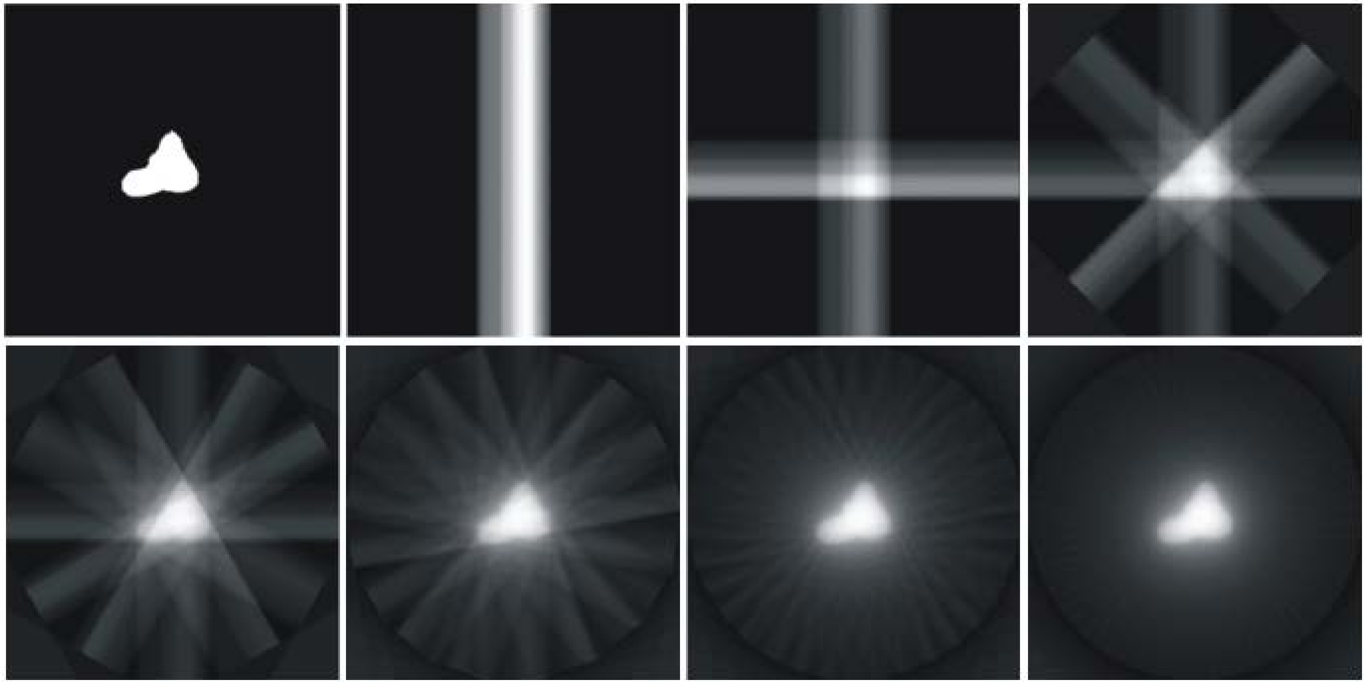

2.4 Number of projections

The number of projections should be in the same order as the number of rays in one projection.
For M projections with N rays over 180° , the angular increment δ between two consecutive projections is given in Fourier space as

$$\delta = \frac{\pi}{M}$$

For distance T between two neighboring rays, the highest measured spatial frequency ω_{max} in the projection is given by Nyquist's Theorem as

$$\omega_{\max} = \frac{1}{2T}$$

This is the radius of a disk in the frequency domain that contains all measured values.
The distance d between two consecutive values on the circle is:

$$d = \omega_{\max} \cdot \delta = \frac{1}{2T} \frac{\pi}{M}$$

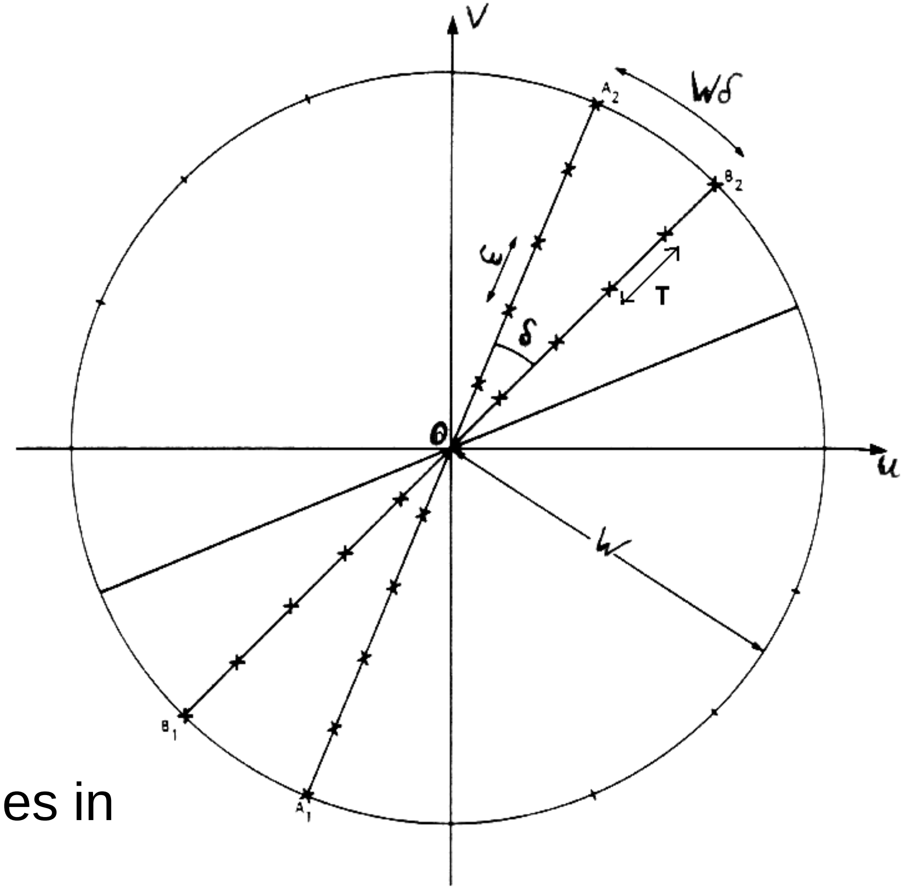

Density of measured values in frequency domain

For N measured values for each projection in spatial domain, there are also N measured values for each measured line in the frequency domain, so that the distance ε between two consecutive measured values on a radial line (or diameter) in frequency domain is given as

$$\varepsilon = \frac{2\omega_{\max}}{N} = \frac{1}{TN}$$

For the worst azimuthal resolution in frequency domain to match the radial resolution, we must demand:

$$\frac{1}{2T}\frac{\pi}{M} \approx \frac{1}{TN}$$

$$\frac{Number\ of\ \ projections}{Number\ of\ \ rays} = \frac{M}{N} \approx \frac{\pi}{2}$$

For practical neutron radiography, most detector systems cannot - at least for sub-millimeter resolution - measure down to the nominal Nyquist resolution given by their pixel size.

The greatest limiting factor is almost always the geometry of the neutron beam and its deviation from the ideal parallel ray model.

Beam optimisation

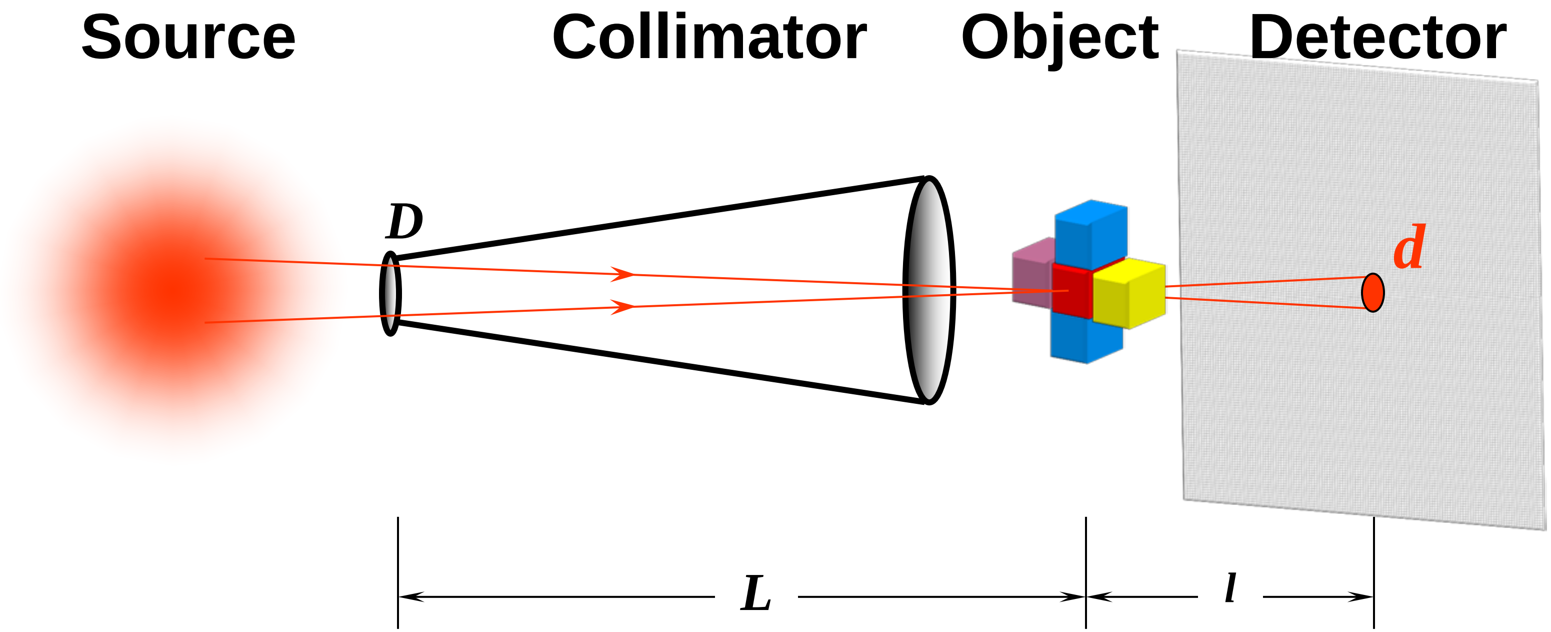

D – Collimator aperture

L – Distance Collimator-Object

l – Distance Object-Detector

$$d = \frac{l}{L/D}$$

Neutron imaging

Beam optimisation

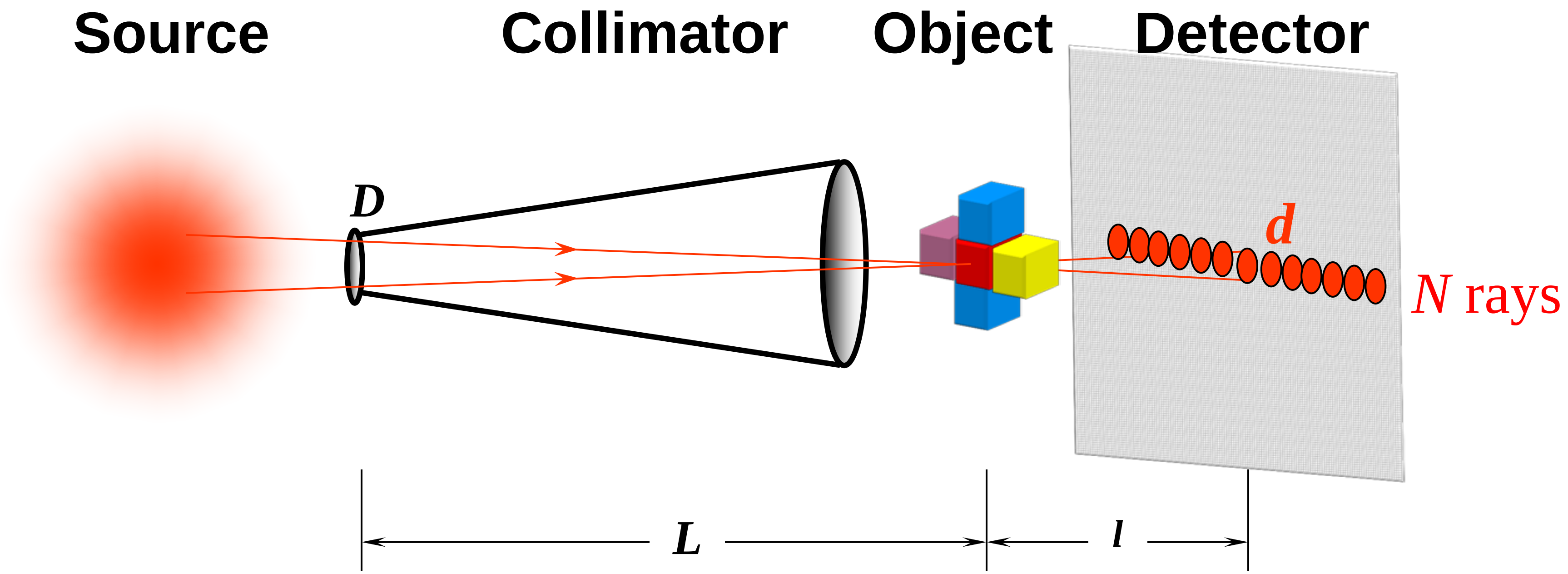

$$M/N = \pi/2$$

$$d = \frac{l}{L/D}$$

Example:
l = 10 cm
L/D = 500
=> d = 0.02 cm

For sample width of 20 cm
N = 1000 => M ~ 1500 projections

For sample width of 2 cm
N = 100 => M ~ 150 projections

Neutron tomography - principle

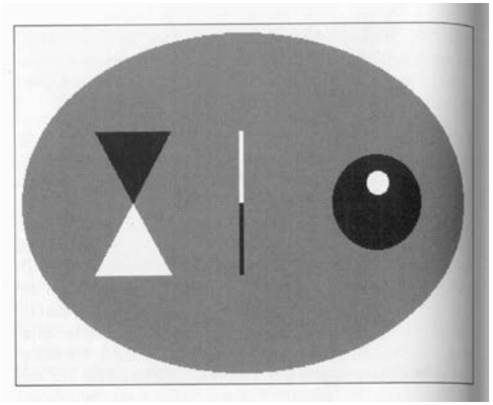

Phantom

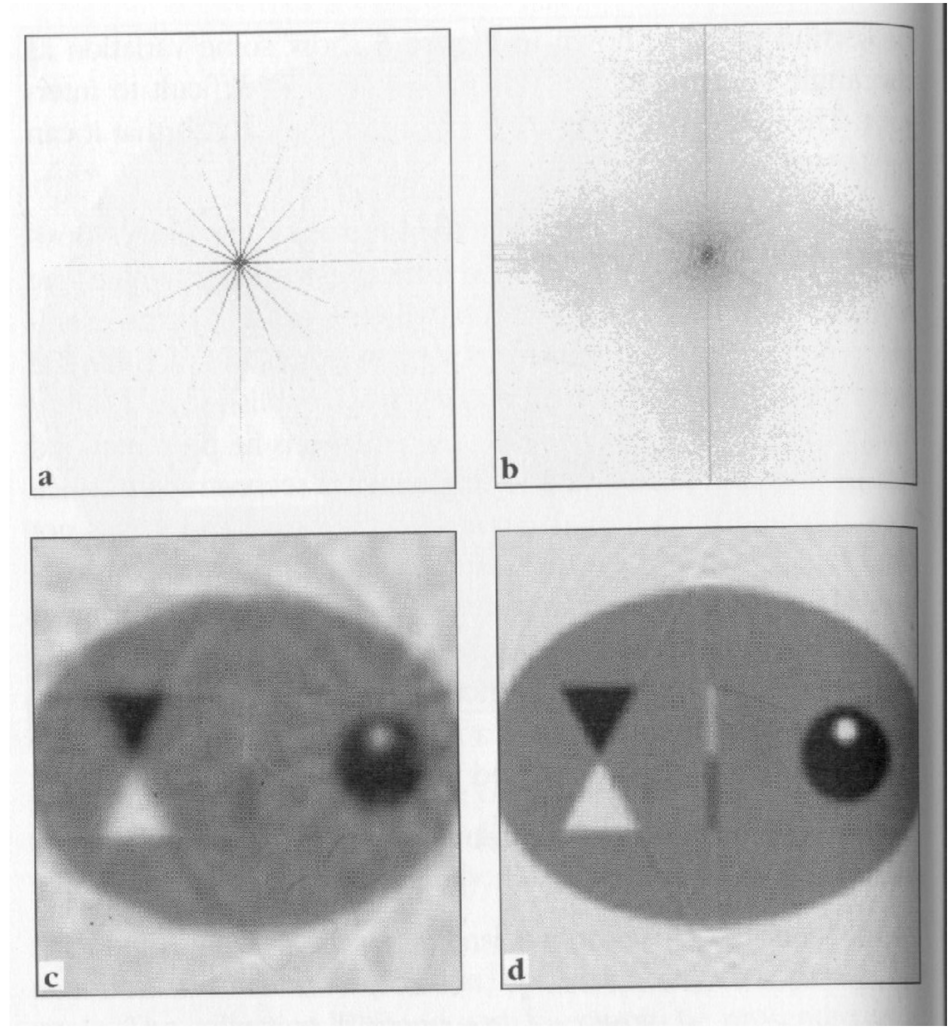

A) 8 views in frequency domain **B) 180 views in frequency domain**

C) reconstruction from image A **D) reconstruction from image B**

Neutron tomography – sinogram preparation

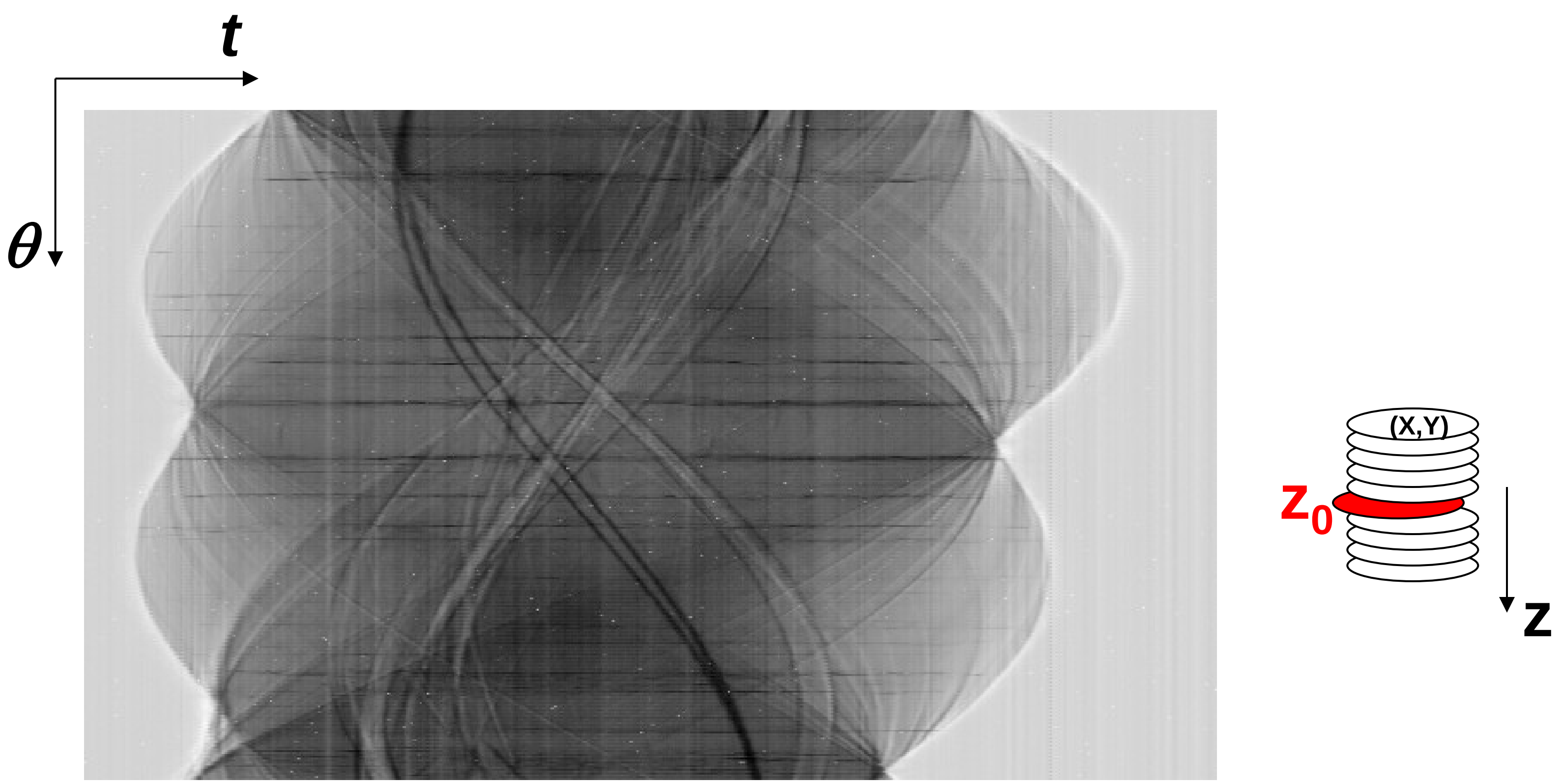

Selecting one z_0 slice from the tomography volume (t,z,θ) and stacking all its projections as a function of the rotating angle theta we will obtain the sinogram, which is used later for the tomography reconstruction.

Attenuation Contrast

Combustion chamber

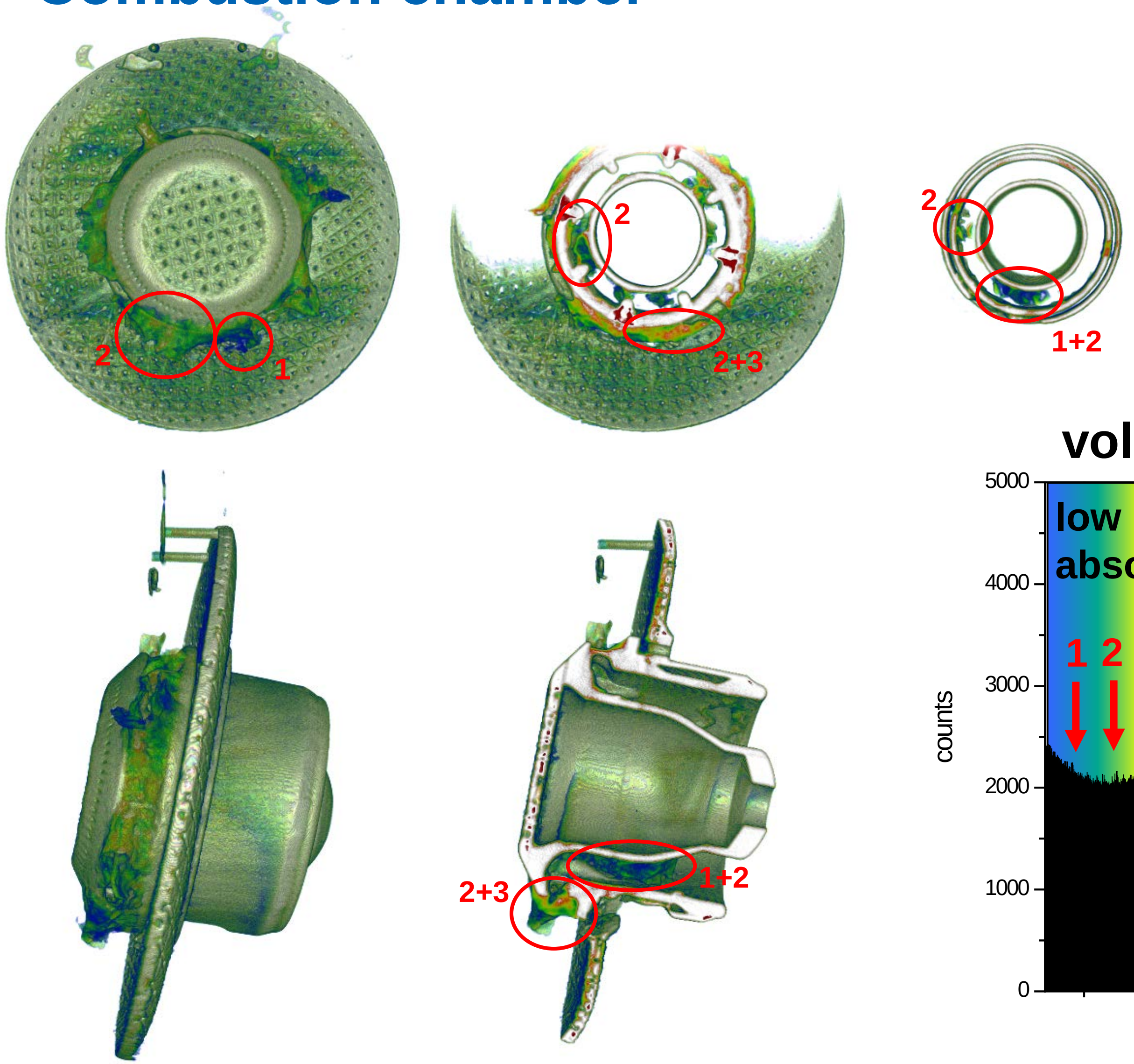

Time scale

1 – old sediments
3 – fresh sediments

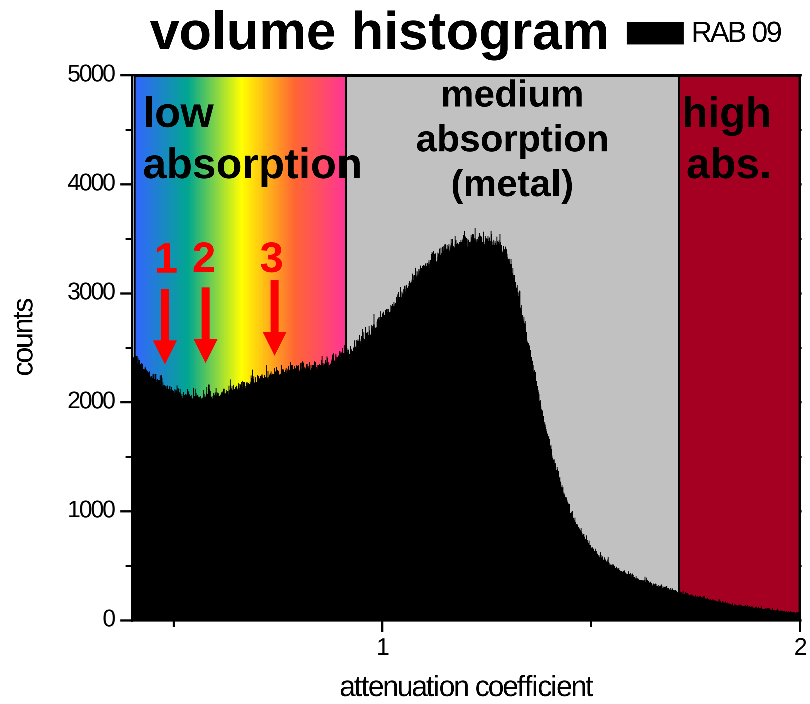

Sample No. 1

Volume sample: 3235 mm^3

Volume impregnation: 0 mm^3

Sample No. 6

Volume sample: 3596 mm^3
Volume impregnation: 639 mm^3

Sample No. 10

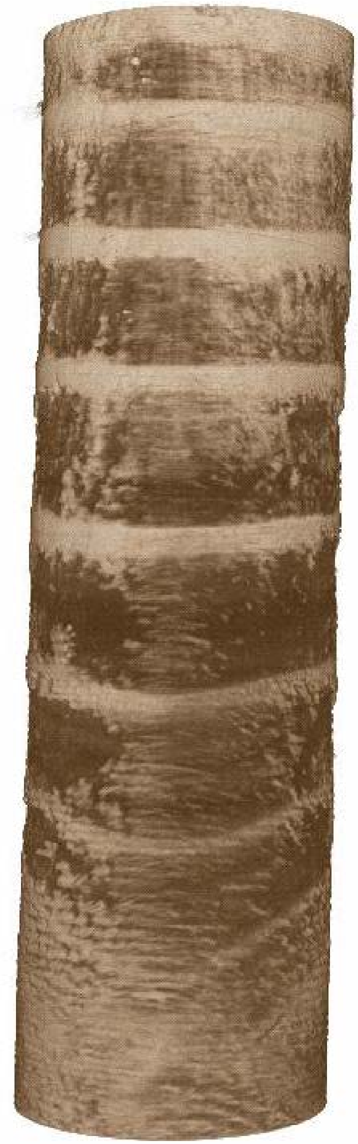

Volume sample: 2989 mm^3
Volume impregnation: 283 mm^3

Particle size distribution in battery, Typ AAA

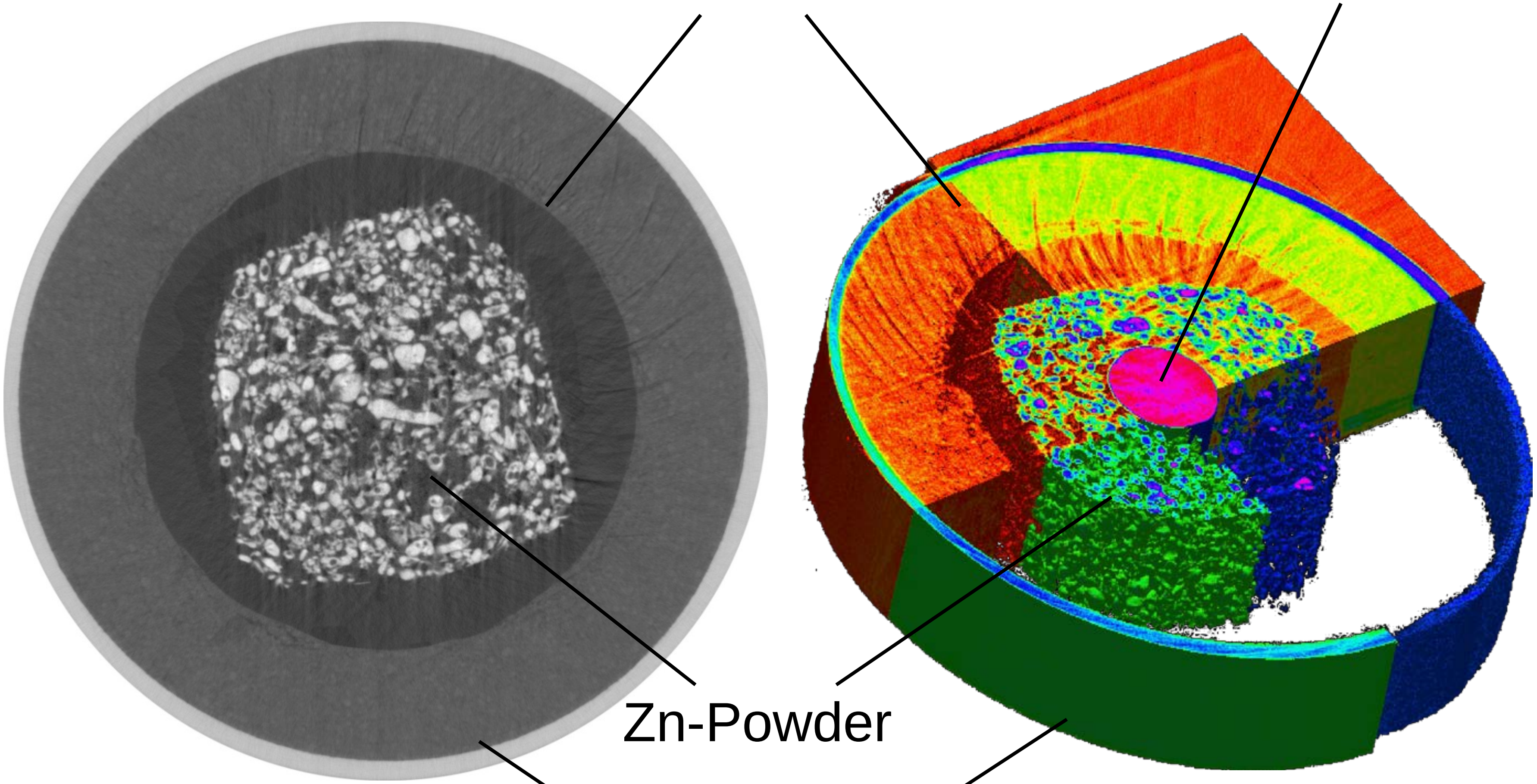

$$Anode$$

$$\begin{aligned} Zn &\rightarrow Zn^{2+} + 2e^- \\ Zn^{2+} + 2OH^- &\rightarrow Zn(OH)_2 \end{aligned}$$

$$Kathode$$

$$\begin{aligned} MnO_2 + H_2O + e^- &\rightarrow MnO(OH) + OH^- \\ MnO(OH) + H_2O + e^- &\rightarrow Mn(OH)_2 + OH^- \ . \end{aligned}$$

Boolean transformation

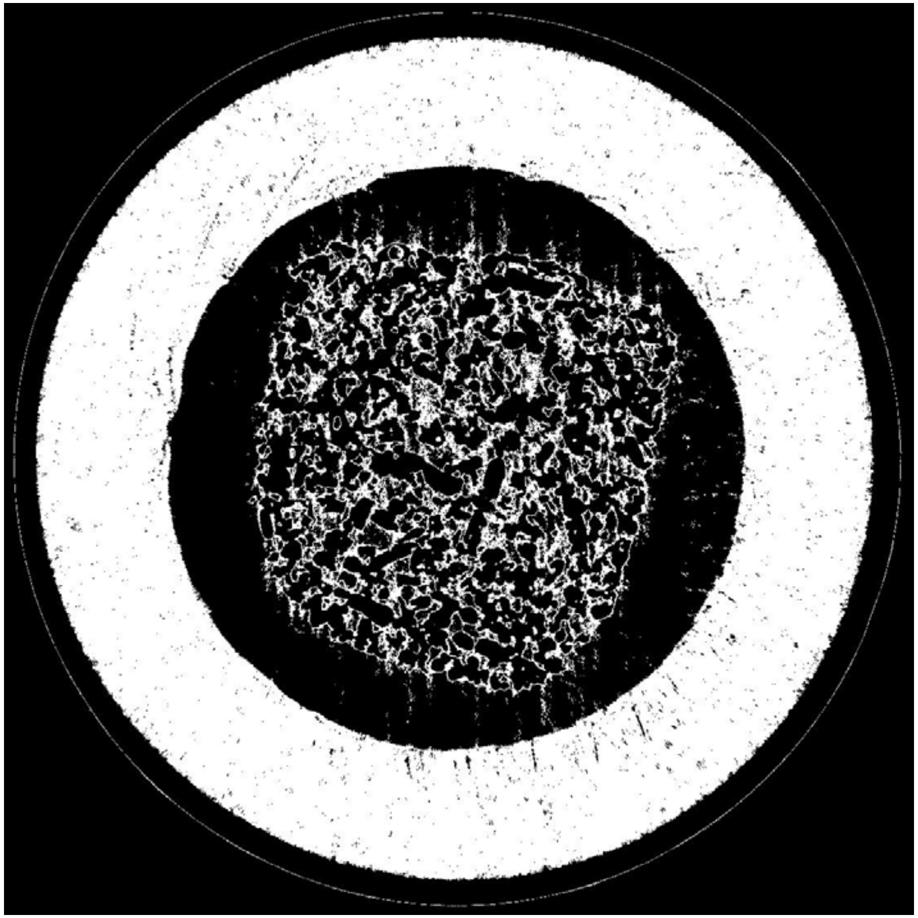

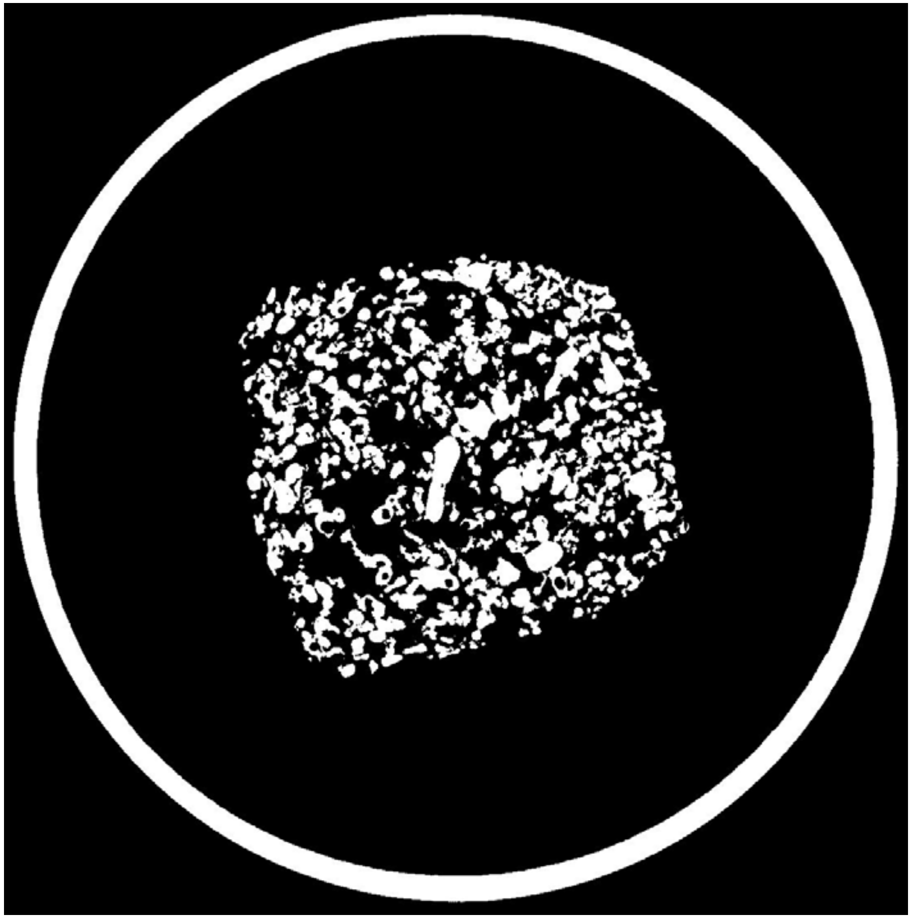

Mn-Ring
Artifacts: Steel case, Powder

Zn-Powder and
Steel case

Morphological transformation

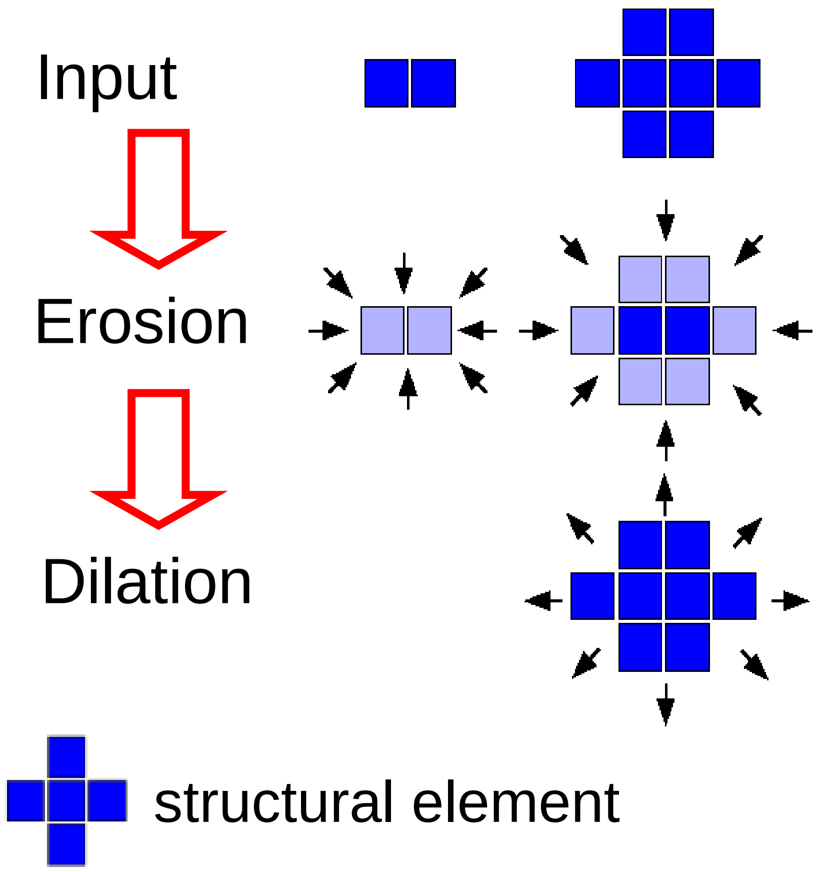

Opening := Dilation + Erosion

Closure := Erosion + Dilation

Noise reduction - Opening process

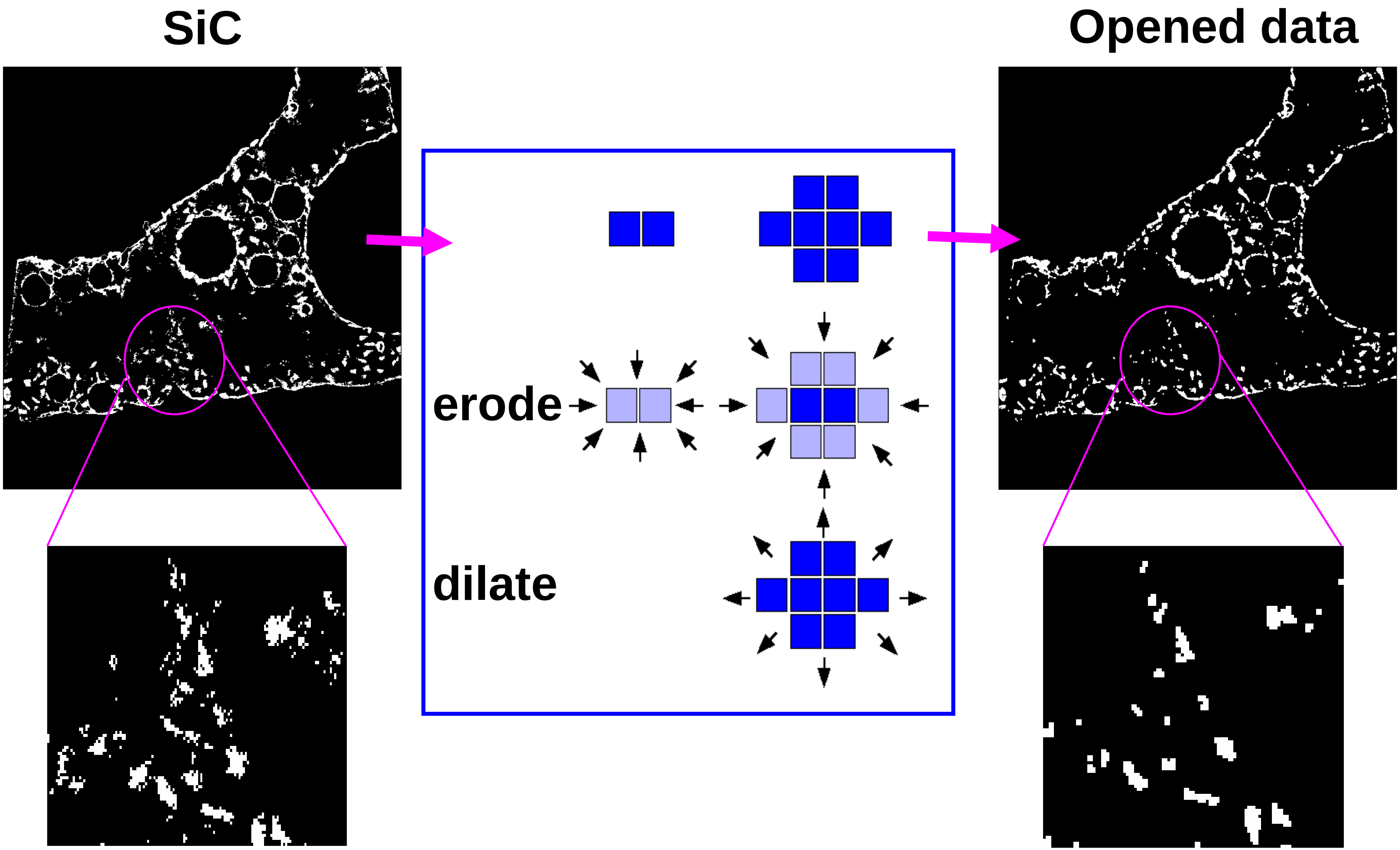

Boolean transformation – intermediate result

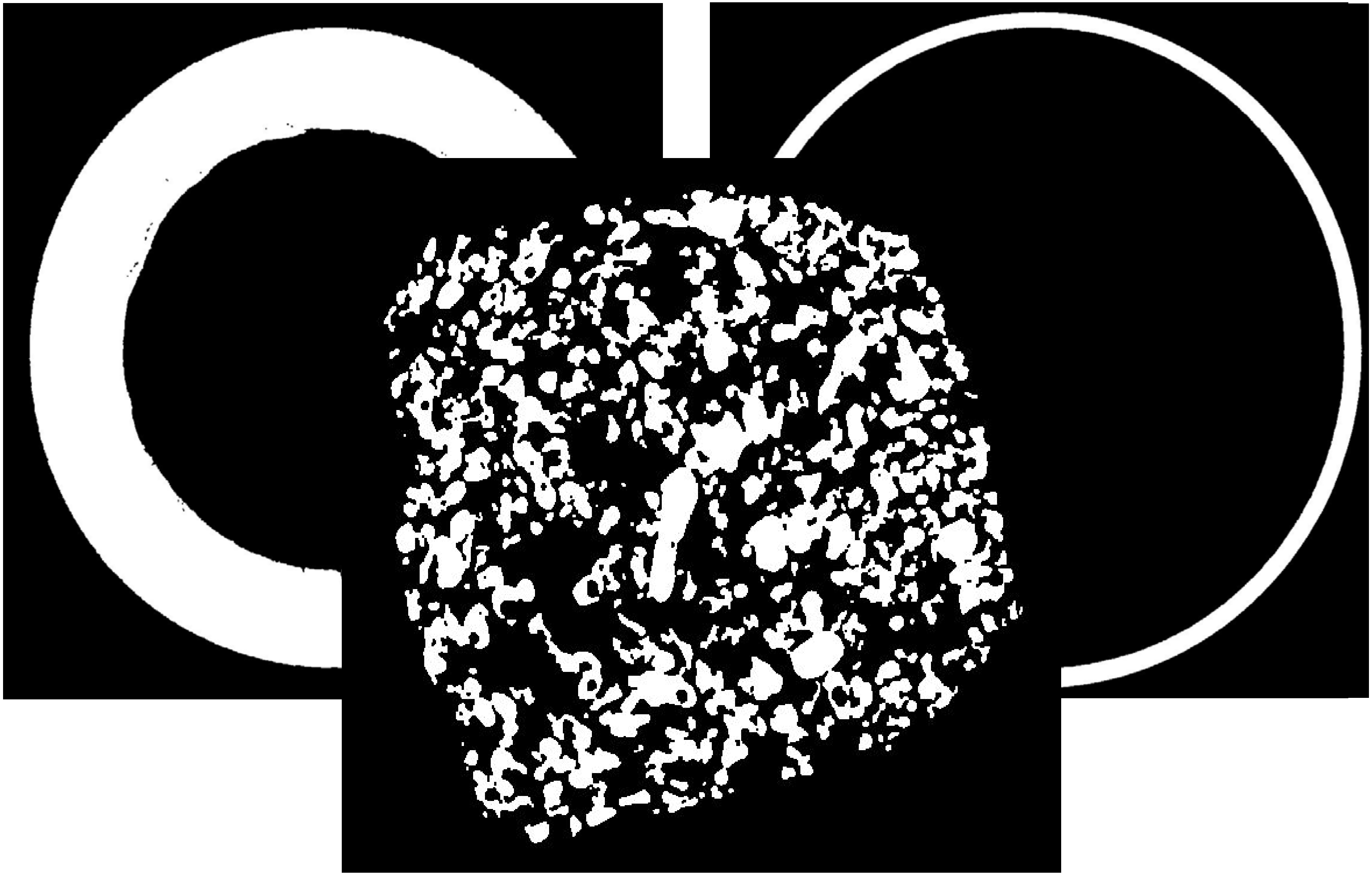

Morphological transformation

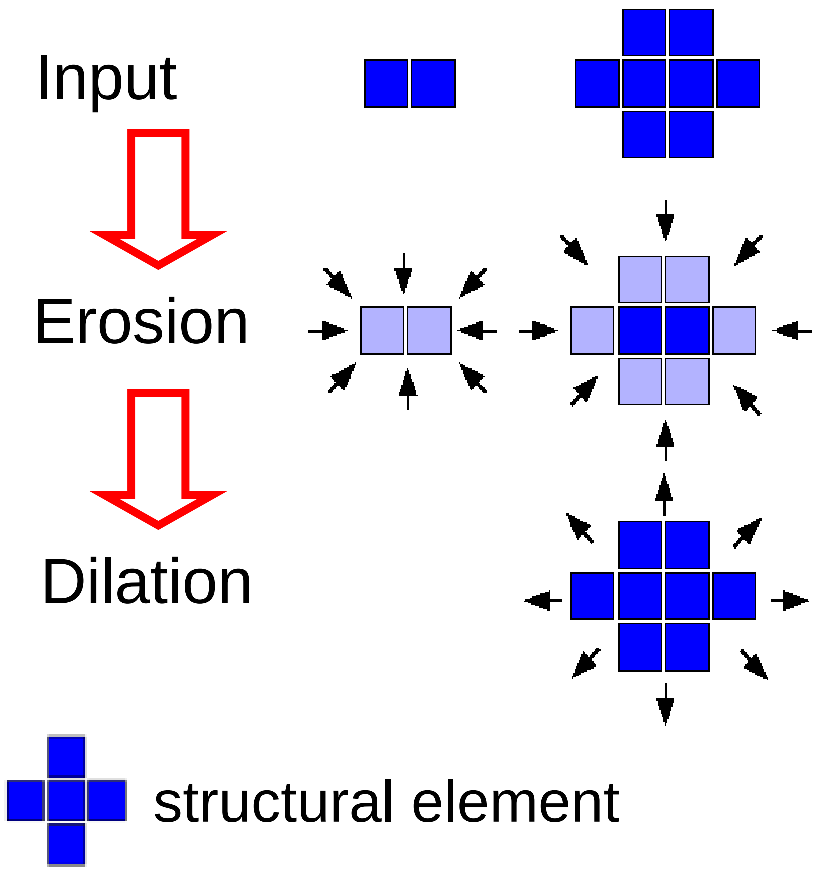

Opening := Dilation + Erosion

Closure := Erosion + Dilation

EDT: Euclid Distance Transformation

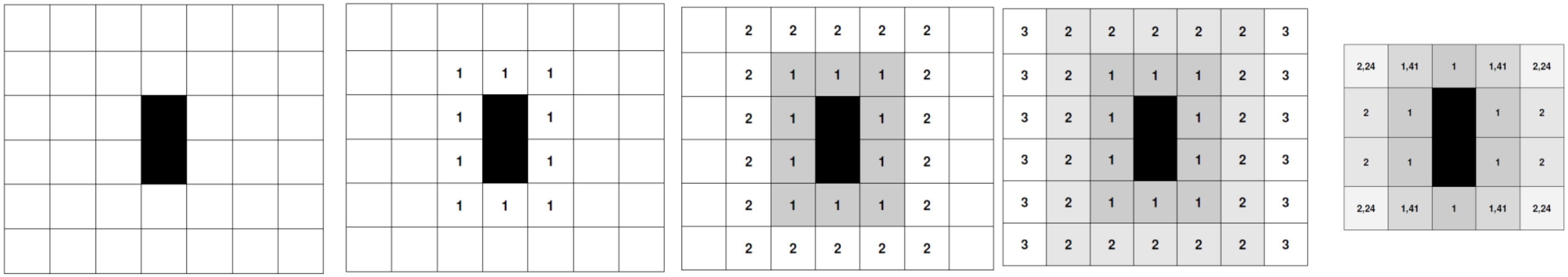

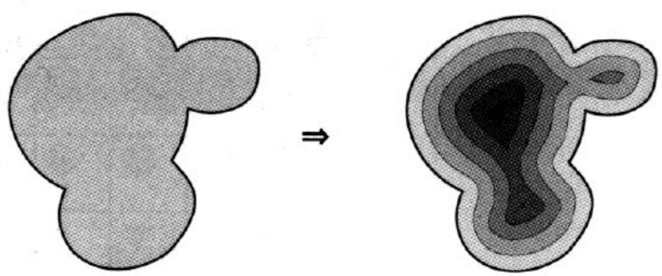

Image: Soille. Morphological Image Analysis. Springer.

Segmentation of powder particles

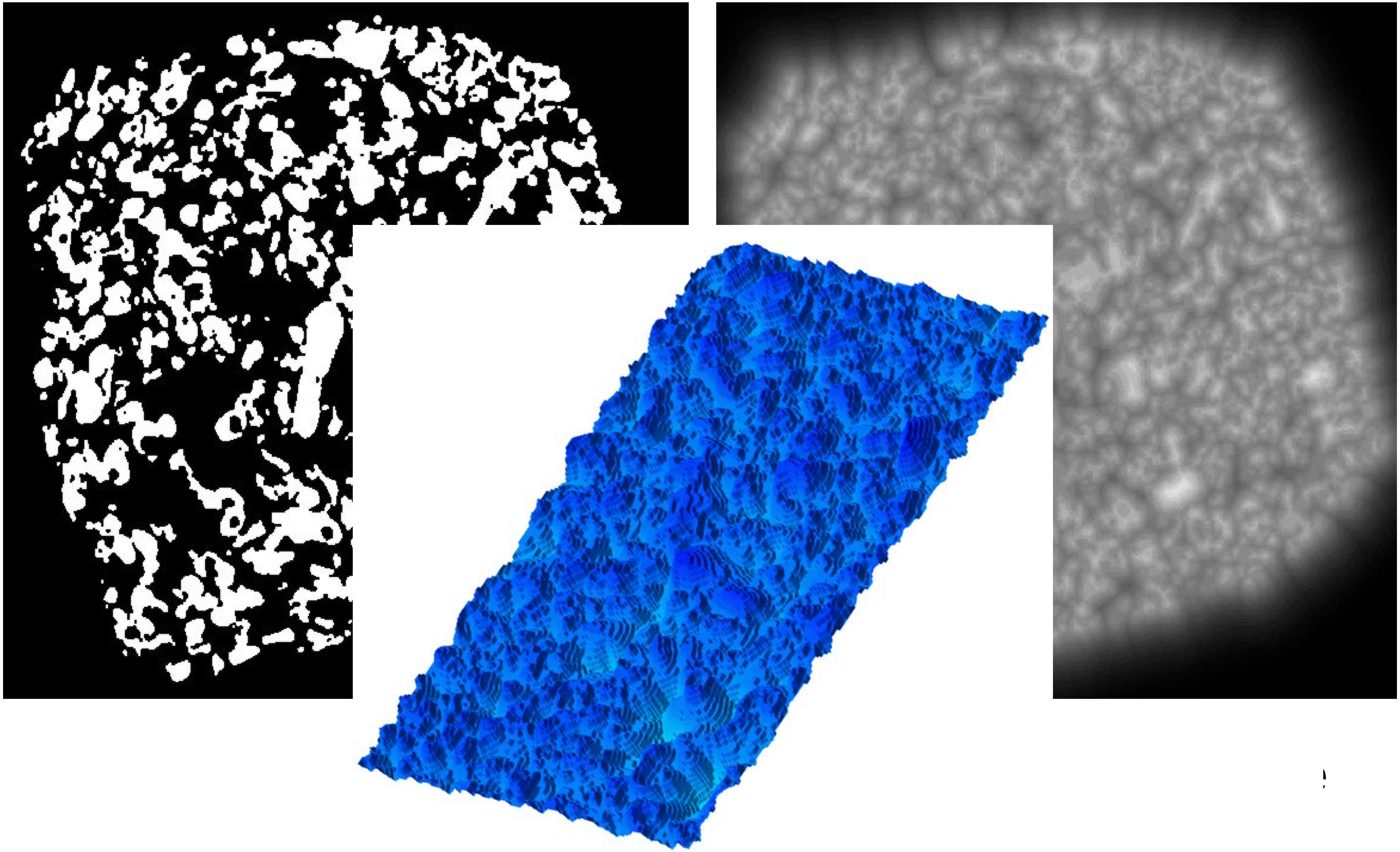

Segmentation of powder particles

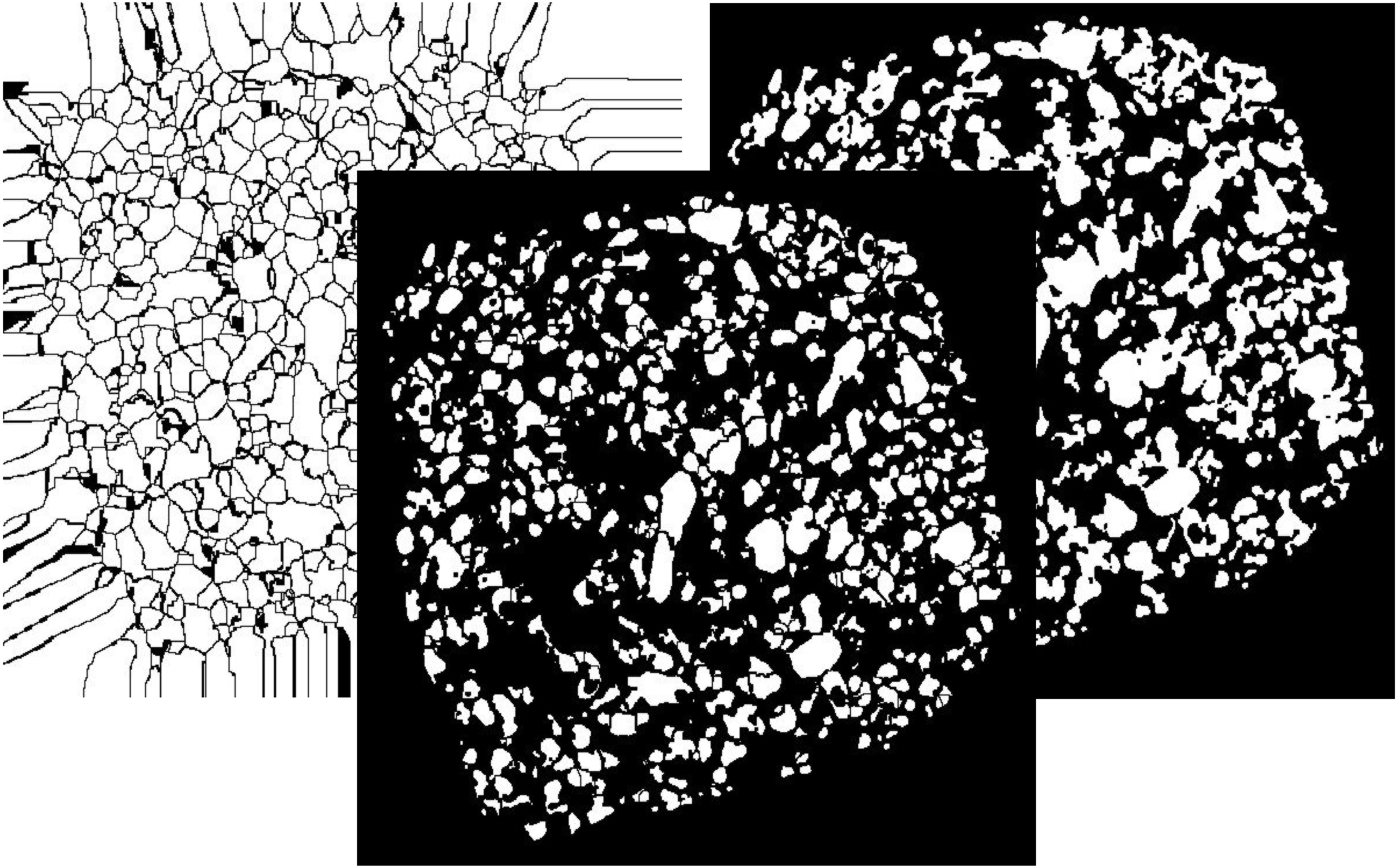

Result – chemical components of the battery

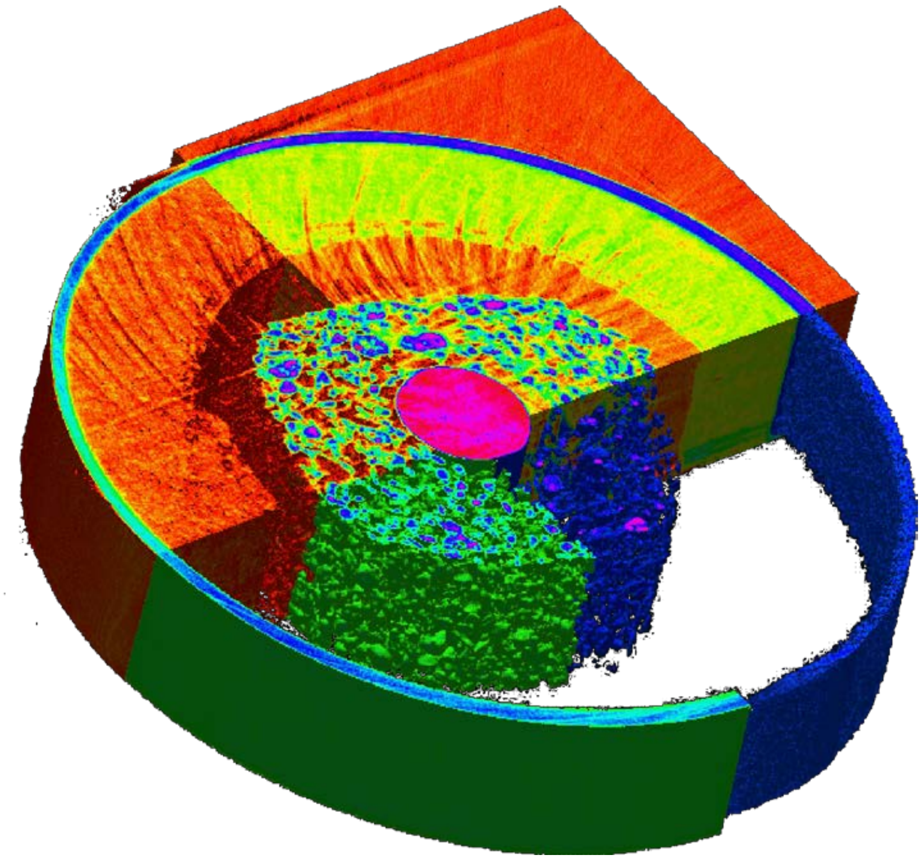

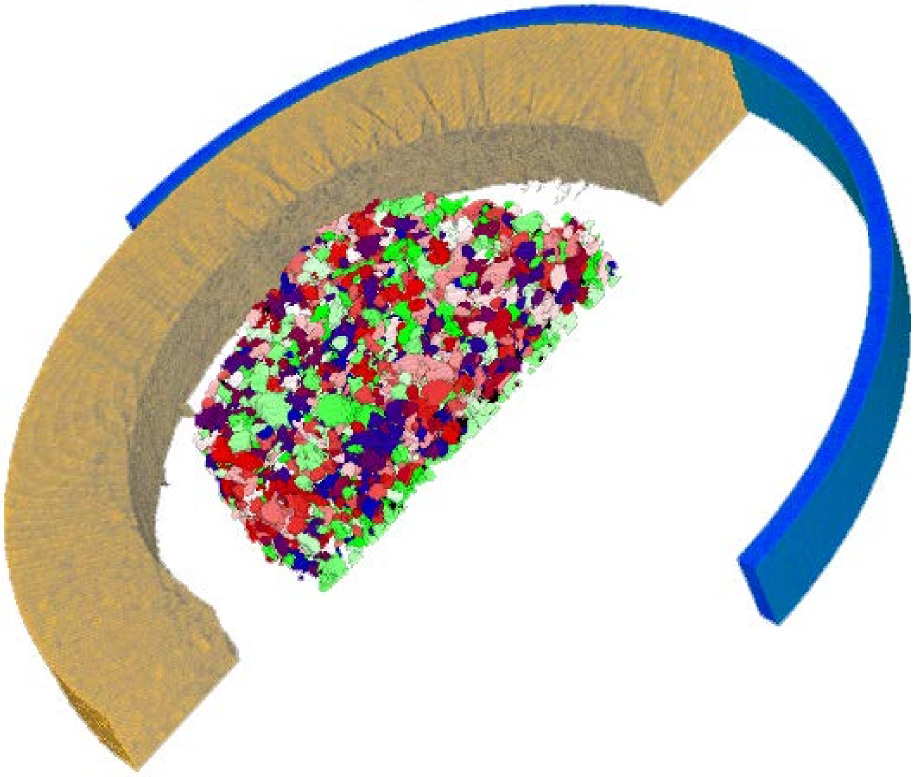

<u>Initial point</u>
3D-Data set

<u>Final result</u>
Multi-component data set

Battery – different discharge levels

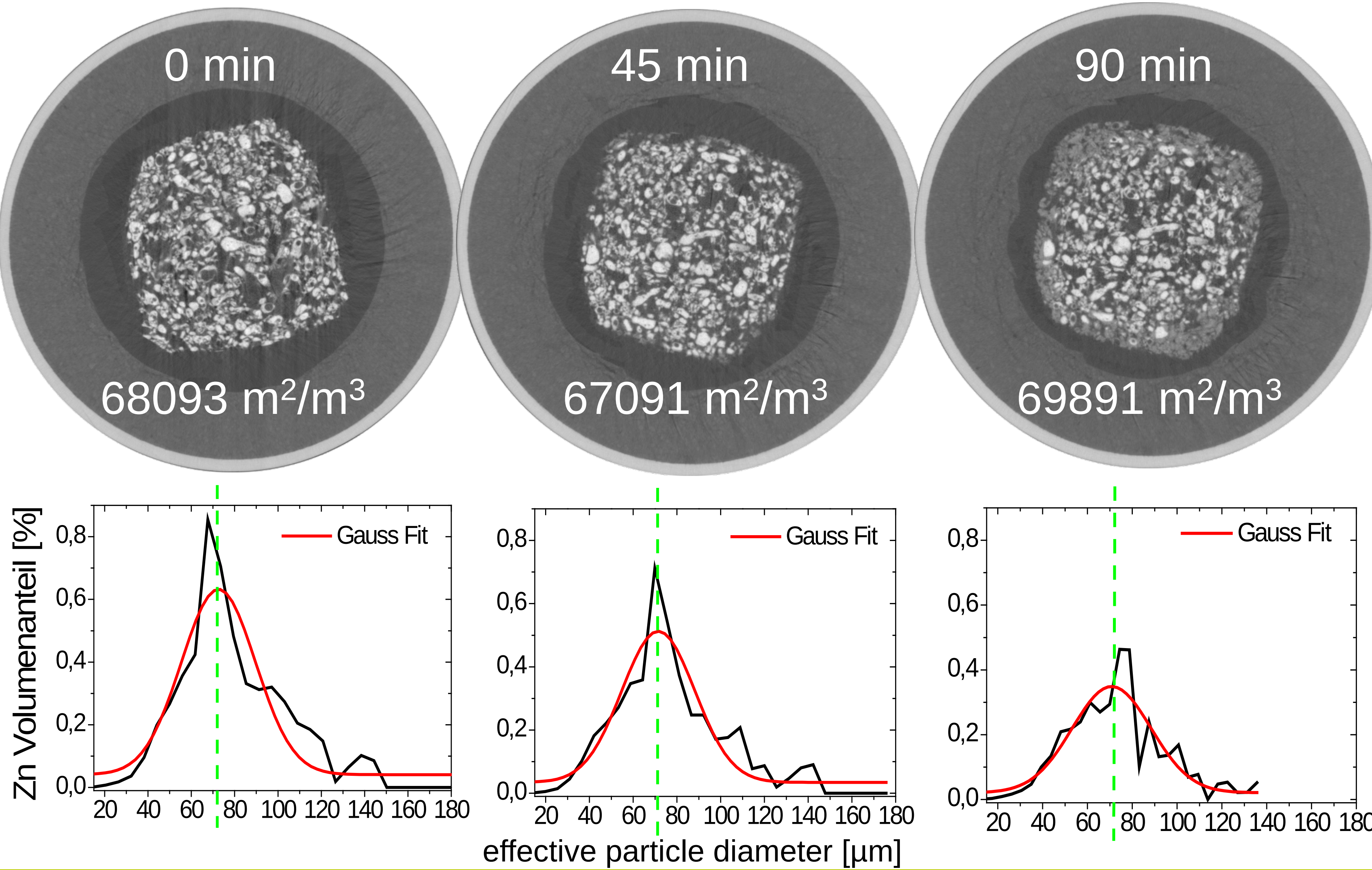


Digital Mummy Project
A Collaborative Effort between
Stanford University
NASA/Stanford Biocomputational Center
Silicon Graphics Inc.
and
The Rosicrucian Egyptian Museum

Thank you !